

Enhanced Performance of Hydrogen Peroxide Modified Pozzolan-based Geopolymer for Abatement of Methylene blue from Aqueous Medium

Dzoujo Tamaguelon Hermann

University of Douala: Universite de Douala

Tome Sylvain (✉ sylvatome@yahoo.fr)

University of Douala <https://orcid.org/0000-0001-9200-7776>

Victor O Shikuku

Kaimosi Friends University College

Jean T Tchuigwa

University of Douala: Universite de Douala

Alex Spieß

Universitat Wien Institut fur Anorganische Chemie und strukturchemie, universitat dusseldorf

Christoph Janiak

Universitat Wien Institut fur Anorganische Chemie und strukturchemie, Universitat dusseldorf

Marie Annie Etoh

University of Douala: Universite de Douala

David Dina

University of Douala: Universite de Douala

Research Article

Keywords: Pozzolan, eco-adsorbents, geopolymers, adsorption, methylene blue

Posted Date: May 19th, 2021

DOI: <https://doi.org/10.21203/rs.3.rs-511676/v1>

License:  This work is licensed under a Creative Commons Attribution 4.0 International License.

[Read Full License](#)

Version of Record: A version of this preprint was published at Silicon on August 10th, 2021. See the published version at <https://doi.org/10.1007/s12633-021-01264-4>.

Enhanced performance of hydrogen peroxide modified pozzolan-based geopolymers for abatement of methylene blue from aqueous medium

Dzoujo T. Hermann¹, Sylvain Tome¹, Victor O. Shikuku², Jean T. Tchuigwa¹, Alex Spieß³, Christoph Janiak³, Marie Annie Etoh¹, David Dina¹

¹Department of Chemistry, Faculty of Sciences, University of Douala, P.O. Box 24157, Douala, Cameroon

²Department of Physical Sciences, Kaimosi Friends University College, P.O. Box 385-50309 Kaimosi-Kenya

³Institut für Anorganische Chemie und Strukturchemie, Universität Düsseldorf, Universitätsstr. 1D-40225 Düsseldorf, Germany, Tel. int+49-211-81-12286

*Corresponding authors: P. Box, +237 697082352, Email: dinadavidcr@yahoo.com ; P. Box 2396, +237 694825926, Email: sylvatome@yahoo.fr

Abstract

Pozzolan-based eco-adsorbents were synthesized by geopolymerization with addition of hydrogen peroxide (H_2O_2) with mass ratios 0% (GP_0) and 1% (GP_1) and the products used to sorb cationic methylene blue (MB) dye from water. The chemical composition, textural properties, mineral composition, surface functions, as well as morphology and internal structure of these samples were determined by the X-ray fluorescence, adsorption of nitrogen by the B.E.T (Bruamer Emmet Teller) method, X-ray diffraction, Fourier Transformed Infrared Spectroscopy (FTIR) and scanning electron microscopy (SEM), respectively. The effects of contact time, dye initial concentration, adsorbent dosage, pH and temperature were examined and are herein reported. Incorporation of 1% H_2O_2 increased the specific surface area from 4.344 to 5.610 m^2/g representing ~29% increase in surface area. This translated an increase in the MB adsorption capacity by 15 orders of magnitude from 24.4 to 366.2 mg/g for GP_0 and GP_1 , respectively. The adsorption rates of methylene blue on the two geopolymers were best described by the pseudo-second order kinetic model. The adsorption equilibrium data were best described by the Sips and Freundlich isotherms models for GP_0 and GP_1 , respectively. Thermodynamically, it was determined that the adsorption of methylene blue onto GP_0 and GP_1 is a physical and endothermic process. The results show that incorporation of low amount of

hydrogen peroxide into pozzolan-based geopolymers increases their adsorption capacity for methylene blue dye stupendously while preserving the surface chemistry.

Keywords: Pozzolan, eco-adsorbents, geopolymers, adsorption, methylene blue

1. Introduction

The problem of environmental pollution is still a topical issue because many industrial activities continue to generate various traditional and emerging pollutants, likely to create significant nuisance such as the destruction of aquatic fauna and flora [1]. Indeed, industrial effluents are among the major sources of environmental pollution. Additionally, these pollutants have the capacity to bioaccumulate along the food chain and accumulate in certain organs of the human body [2]. It is therefore essential to eliminate these toxic elements present in the industrial effluents or to reduce their concentrations below the admissible thresholds defined by the stipulated standards [1]. Faced by increasingly restrictive regulations, industries must obligatorily treat their effluents before discharging into the environment. To fight against this environmental issue, research in identification and elimination of water pollutants, such as methylene blue, directly involved in the appearance of imbalances in ecosystems like photosynthesis inhibition, under oxygenation, bioaccumulation or inducing serious disorders that can harm health such respiratory problems or even lead to death, both in animals and humans, is ever increasing [3].

For this purpose, various classical pollutant removal techniques are used namely coagulation, flocculation, filtration, advanced oxidation processes (AOPs) and adsorption onto activated carbons. Though traditional approaches are insufficient in removing dyes from water to molecular levels, advanced oxidation processes are very expensive and toxic by-products are formed in the process of dye removal [4]. On the other hand, activated carbon is very expensive and the cost of regeneration is also very high [5]. The development of eco-friendly and cost-effective technologies are more and more desired to preserve the environment and for sustainability, respectively. Among the different treatment processes of dye-containing water effluents, adsorption stands out to be one the techniques relatively easy to use, easy to set up and of diverse variety of adsorbents that can be used such as: biomass-derived activated carbons, clays and pozzolans among others [6]. The latter is an abundant and inexpensive natural resource in the world. Cameroon is counted among the largest producers of natural pozzolan, producing approximately 600 Kt/year [7]. It consists mainly of oxides of silicon, aluminum

and iron (SiO_2 , Al_2O_3 and Fe_2O_3) [8]. Pozzolan is used as a raw material in cement plants and in water treatment [9, 10]. However, its use in the field of adsorption is still limited due to its low adsorbing power, relative to other adsorbents [10]. For judicious use of this natural resource, its adsorption characteristics must be improved. Several works on the synthesis and adsorption of industrial contaminants onto geopolymers based on clays and fly ashes have been reported in literature [11-13]. These studies demonstrate the efficiency of geopolymers in the elimination of dyes from water effluent. However, the rarity of industrial waste precursors in many developing countries especially in remote areas, relative to pozzolan, limit their exploration. The transformation of the pozzolan into amorphous zeolite (geopolymer) is a sustainable and inexpensive way for its utilization as adsorbent for water treatment. Geopolymerization only does not guarantee a high adsorbing product [14]. Consequently, several additives have been evaluated for amelioration the adsorption characteristics of geopolymers. Singhal et al. [15] reported the use of Cetyl trimethylammonium bromide (CTAB) to improve the textural characteristics of metakaolin-based geopolymer. Other approaches include the chemical modification using bivalent metallic ions such as nickel, zinc and barium [16, 17]. These methods have their inherent limitation. CTAB is not only expensive but also changes the surface chemistry of the geopolymer. Alteration of the constitution of the geopolymer introduces site specific interactions that may induce specificity in the uptake of pollutants. Additionally, incorporation of bivalent heavy metals may cause secondary water pollution in case of leaching from the geopolymer framework. Simple, low-cost and environmentally benign methods are required for ameliorating the textural and adsorption characteristics of geopolymers. Hydrogen peroxide is known to decompose quickly in alkaline solution, the preparation conditions for geopolymer synthesis. The oxygen so-generated could be trapped in the geopolymer structure thus improving its porosity parameters and hence its adsorption performance while preserving its surface chemistry. The objective of this work was to ameliorate the adsorption characteristics of pozzolan-based geopolymers by preparation of a hydrogen peroxide modified pozzolan-based geopolymer as an eco-adsorbent. The effects of incorporation of hydrogen peroxide on the textural, structural and adsorptive performance for the removal of methylene blue dye from aqueous solution under various experimental conditions were examined and are herein reported.

2. Materials and Methods

2.1 Geopolymer synthesis

The pozzolan used as a source of aluminosilicate was obtained from the locality of Mbrououkou in the Littoral region of Cameroon, crushed and sieved through 100 μ m sieve to obtain uniform particle size. The alkaline activator solution was prepared by blending the sodium hydroxide (12M from 98% purity sodium hydroxide flake) and commercial water glass (28.7 wt.% SiO₂, 8.9 wt.% Na₂O and 62.4 wt.% H₂O; density 1.37 g/mL). The ratio (liquid/liquid) of sodium hydroxide/commercial water glass was 2.4. The geopolymer was synthesized by mixing the alkaline solution and the pozzolan powder in a liquid/solid ratio of 0.3. This blend was homogenized for 10 minutes using a mixer where a fresh paste was formed. To alter the porosity of the geopolymers, hydrogen peroxide in a mass ratio of 1% was added, as a blowing agent, to the paste previously left to rest for 30 minutes and it was then poured into cylindrical PVC moulds. Once moulded, the whole was mechanically compacted for one minute and then put in an oven (MEMMERT B2162385) at 60°C for 24 hours, then removed and left to rest for 4 days. The geopolymer samples obtained without (pristine) and with incorporation of hydrogen peroxide labeled GP₀ and GP₁, respectively, were then dipped in acetone for 2 hours to stop the geopolymerization process, then dried in the oven at 60°C for one hour. They were then crushed, sieved and washed until a neutral pH is obtained, then dried in an oven for 6 hours.

2.2 Materials Characterization

The pozzolan and the synthesized geopolymers were subjected to various physico-chemical characterizations in order to determine chemical composition, textural properties, mineralogical composition, surface functional groups, internal structure and morphology by the following methods:

2.2.1 X-ray fluorescence

The x-ray fluorescence spectrometry (XRF) method (Bruker-SRS 3400) was used to determine the bulk oxide composition of pozzolan.

2.2.2 Iodine and methylene blue indices

The iodine and methylene blue indices are determined following the method used by Mbaye [18] to evaluate the microporosity and macroporosity of eco-adsorbents. The procedures are as follows:

2.2.2.1 Iodine Index

In a 100 mL Erlenmeyer flask, 0.1g of geopolymers previously dried in an oven at 110°C for 24 hours were brought into contact with 20 mL of 0.02N iodine solution mixture stirred for 4

to 5 min and then filtered. Subsequently, 10 mL of the filtrate was titrated with sodium thiosulfate solution (0.1 N) using starch as the color indicator.

2.2.2.2 Methylene Blue Index

In a 100 mL Erlenmeyer flask, 0.1g of previously dried geopolymers and 50 mL of methylene blue solution were mixed, and the mixture stirred for 4 to 5 minutes and then filtered. The residual methylene blue concentration was determined using a UV - visible spectrophotometer (MERCK spectroquant Pharo 300 UV/visible instruments) at a wavelength of 662 nm.

2.2.3 The point of zero charge (pH_{PZC})

The point of zero charge was determined following the protocol described by Karadag (2007) [19]. Briefly, six NaCl control solutions (0.1M) with a pH between 2 and 12 are prepared. To 20 mL of each of these solutions is added 0.1g of adsorbent. The suspensions obtained are left to stand for 8 hours under stirring at room temperature, and their pH values are accurately determined using a pH meter (VOLTCRAFT PH-100ATC) after filtration.

2.2.4 Nitrogen Adsorption and Surface Area Measurement

Total surface area and micropore surface area of powder geopolymers were determined using N₂ adsorption at 77 K in a Quantachrome Autosorb AS6AG Station 3 instrument (Institute of Inorganic chemistry and structural of Dusseldorf, Germany). The values of the two properties were calculated from experimental isotherms using the Brunauer-Emmett-Teller (BET) analysis method.

2.2.5 X-ray Diffraction

The crystalline phases present on the samples were determined using X-ray diffraction (XRD). An X-ray Powder Diffractometer (Bruker D8 Discovery, US) with the Bragg-Bretano theta-theta configuration, using a CuK α radiation at 27.5 kV and 25 mA was used for characterization. Spectra was obtained in the 2 θ range from 6° to 80° with a step of 0.02° and 1 second per step scan rate.

2.2.6 Scanning Electron Microscopy

Microscope equipped with Energy Microstructure analysis was carried out in some selected specimens by HITACHI S-3400N Scanning Electron Dispersive X-ray Spectrometry analysis (EDS), operating at 15.0 kV.

2.2.7 Fourier Transform Infra-Red spectroscopy (FTIR)

Fourier Transform Infra-Red spectroscopy (FTIR) permits the identification of functional groups on the surface of these materials. FTIR analysis of the samples was carried out by a FTIR Spectrophotometer (Nicolet 5700 FTIR, Thermo Electron Corporation) between 4000 and 400 cm⁻¹ wavenumbers.

2.3 Adsorption experiments

Methylene Blue (MB) ($C_{16}H_{18}ClN_3S_xH_2O$) solutions were prepared at pre-defined concentrations for adsorption experiments.

The adsorption experiments were carried out in batches at different initial values of dye concentrations (10, 20, 30, 40 and 50 mg/L) and contact time using a precisely weighed quantity of adsorbents (0.1g) into a 50 mL diluted solutions. After equilibration of 30 minutes for GP₁ material and 50 minutes for the GP₀ material, the absorbance of residual solutions was measured using a spectrophotometer (MERCK spectroquant Pharo 300 UV/visible instruments) at a wavelength of the MB (662 nm).

The adsorption capacity at a given time and the percent removal (%R) of methylene blue were calculated using the following equations:

$$q_t = \frac{(C_0 - C_t)V}{m} \quad (1)$$

$$R(\%) = \frac{(C_0 - C_t) \times 100}{C_0} \quad (2)$$

Where:

q_t : The quantity adsorbed at time t (mg/g); C_0 : The initial dye concentration (mg/L);

C_t : The dye concentration at time t (mg/L); V: The volume of the solution (mL) and

m: The mass of the adsorbent in solution (g).

2.3.1 Effect of contact time

The tests were carried out by mixing in a reactor, in turn, 0.1 g of each geopolymer with 50 mL of the MB solution with a concentration of 50 mg/L. The homogenization of the mixtures is ensured by a magnetic stirrer at a stirring rate of 120 rpm during time intervals of 10, 20, 30, 40, 50 and 60 minutes.

2.3.2 Effect of the initial concentration

Diluted methylene blue solutions of 50 mL at different concentrations (10, 20, 30, 40 and 50 mg/L) were prepared and introduced into 5 reactors. A mass of 0.1 g of different geopolymers was added to each of these reactors and the mixture was stirred until the fixed equilibrium times

of 30 minutes for GP₁ material and 50 minutes for the GP₀ material, respectively, filtered and residual MB determined.

2.3.3 Effect of pH

The effect of pH was examined by varying the pH of the MB solution from 2 to 12 using a solution of hydrochloric acid HCl (0.1N) or caustic soda NaOH (0.1N) depending on the desired pH.

2.3.4 Effect of adsorbent dosage

To various MB solutions with a concentration of 50 mg/L, masses of 0.05, 0.1, 0.2, 0.3, 0.4 and 0.5 g of each geopolymers, singly, was added and stirred at time intervals of 30 minutes for GP₁ material and 50 minutes for the GP₀ material. Subsequently, the different samples were filtered and residual MB concentration determined.

2.3.5 Effect of temperature

A fixed mass (0.1 g) of different geopolymers was added to 50 mg L⁻¹ of MB solutions (50 mL). The temperatures were adjusted between 309-339 K and the contents agitated until equilibration (30 minutes for GP₁ material and 50 minutes for the GP₀ material) and the residual dye concentration in solution determined.

3. Results and Discussion

3.1. XRF analysis

The chemical composition of pozzolan, as determined by XRF analysis, is presented in Table 1. The main oxides in pozzolan are SiO₂, Al₂O₃ and Fe₂O₃ constituting 75.98%. Considering the potential reactivity of these oxides, the pozzolan was considered suitable for the development of geopolymers [20].

Table 1. Chemical composition of pozzolan (Pz).

Oxides	SiO ₂	Al ₂ O ₃	CaO	Fe ₂ O ₃	Na ₂ O	K ₂ O	MgO	Cl	SO ₃	LOI
Pz (%)	47.74	15.36	8.25	12.88	3.62	1.11	6.45	-	-	0.66

3.2 Textural Properties

3.2.1. Diameter, pore volume and specific area

Table 2 shows the results from the analysis of N₂ adsorption-desorption isotherm curves (Figure 1) as well as the iodine and methylene blue indices. It can be seen that the addition of hydrogen peroxide, which decomposes into water molecules and oxygen during synthesis, appreciably increased the specific surface area, as well as the total pore volume within the material from

4.344 to 5.610 m²/g and 6.022 to 9.747 ($\times 10^{-3}$ cm³/g) for GP₀ and GP₁, respectively. The low values of iodine (444.150 m/g for GP₀ material and 571.050 m/g for GP₁ material) and methylene blue (20 m/g for GP₀ material and 23.680 m/g for GP₁ material) indices indicate that these geopolymers are very mesoporous. This is confirmed by the pore diameters (respectively 105.800 and 103.700 Å for GP₀ geopolymer and GP₁) which are between 2 and 50 nm) [21]. In addition, these both samples have displayed a characteristic type IV nitrogen adsorption–desorption isotherm in accordance with the IUPAC scheme of classification, as shown in Figure 1[22]. Hysteresis loop in the P/P₀ range of 0.4–0.9 denotes the presence of mesopores (pores in the range of 2–50 nm). The slight variation in the N₂ adsorption–desorption isotherms from standard type IV isotherm could be related to the existence of hetero-sized pores [23].

Table 2: Physical properties of the different geopolymers

Adsorbents	Pores volume ($\times 10^{-3}$ cm ³ /g)	total Pores diameter (Å)	specific surface (m ² /g)	Iodine number (m/g)	MB number (mg/g)	pHPZC
GP ₀	6.022	105.800	4.344	444.150	20.000	7.5
GP ₁	9.747	103.700	5.610	571,050	23.680	7.5

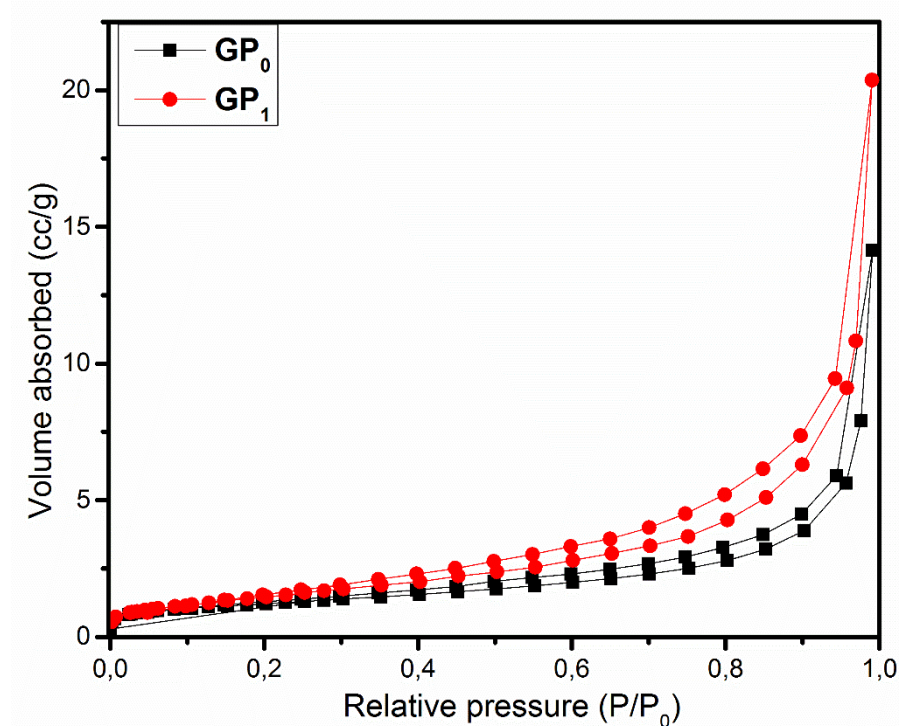


Figure 1: N₂ adsorption-desorption isotherms of eco-adsorbents materials

3.2.2. Point of zero charge pH_{PZC}

As for the pH at the point of zero charge (Figure 2), it can be seen that the different geopolymers have the same pH_{PZC} (7.5). These values are comparable to those reported by Sarkar [16] for an alkali-activated Linz Donawitz (LD) slag. However, it also suggests that the incorporation of hydrogen peroxide during synthesis did not affect the surface functional groups. At solution pH values below the pH_{PZC}, these materials carry a net positive surface charge and a net negative surface charge at pH values higher than the pH_{PZC} [24].

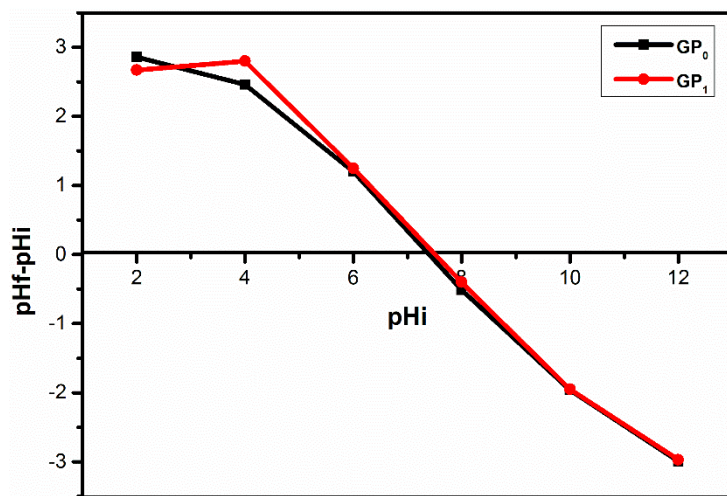


Figure 2: Point of Zero Charge of geopolymer materials.

3.3 Functional groups analysis by FTIR

The FTIR spectrum in figure 3 shows the vibration bands of the different materials recorded between 4000 and 400 cm⁻¹. The pozzolan presents the following vibration bands: the first one between 3550-3400 cm⁻¹ corresponds to the elongation vibrations of the O-H bonds of water molecules [25]. The band around 1650 cm⁻¹ is attributed to the deformation vibrations of the H-O-H bond of water molecules [26]. The bands centered between 1045-977 cm⁻¹ corresponds to the symmetrical and asymmetrical elongations of the Si-O-Si and Si-O-Al bonds [27]. The bands between 913-736 cm⁻¹ is related to the symmetrical vibrations of the Al-O and Al-OH. The bands around 550 and 460 cm⁻¹ correspond to the symmetrical elongations of Si-O-Si, Al-O-Al, Si-O-Fe and deformations of the Si-O-Si, O-Si-O bonds, respectively. Comparing the spectrum of the precursor (Pz) with those of the geopolymers (GP₀ and GP₁), it is observed a shift of the main band of aluminosilicates from ~1023 to ~1036 cm⁻¹. This shift reflects a restructuring of the aluminosilicate phases present in the Pz material. It is also observed a

decrease in intensity of the bands of aluminosilicates (1023 cm^{-1}), silicates (760 cm^{-1}) and ferrates (436 cm^{-1}). This phenomenon confirms the dissolution of these phases in alkaline medium [28].

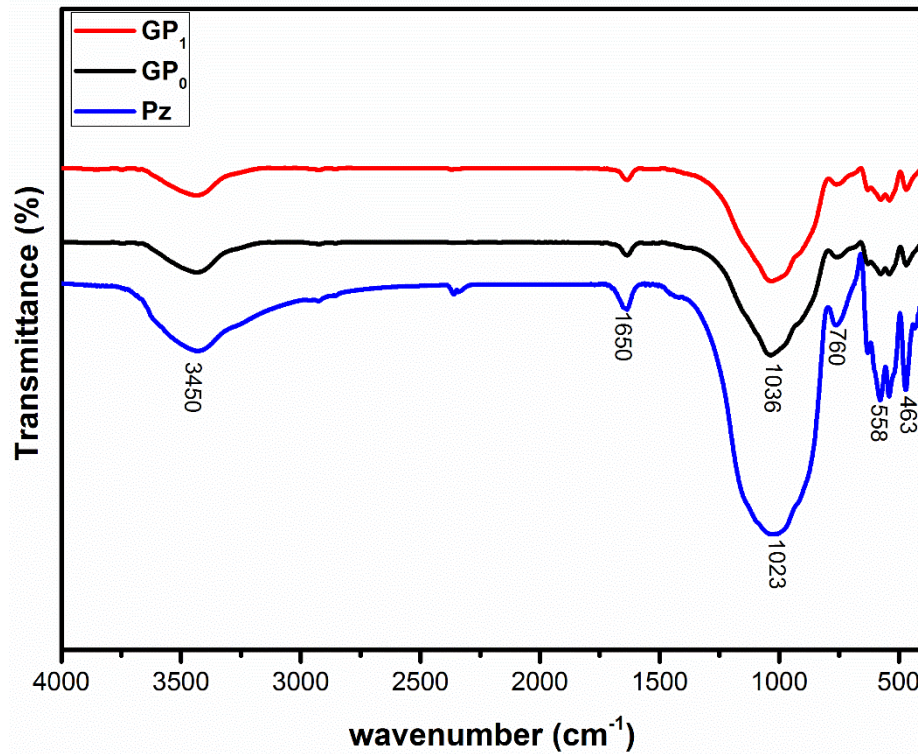


Figure 3: FTIR of the samples Pz, GP₀ and GP₁

3.4 X-ray diffraction analysis (XRD)

The diffractograms of the two studied geopolymers GP₀ and GP₁ and aluminosilicate source (Pz) used for their synthesis are shown in figure 4. The precursor is made in anorthite (An), Na(AlSi₃O₈) (PDF#01-073-6461), feldspar-Na(F), (NaAlSi₃O₈) (PDF#01-083-6911), forsterite (Fs), (Mg₂SiO₄) (PDF # 85-1462), diopside sodian (Ds), Ca(Mg, Fe, Al)(Si, Al)₂O₆ (PDF#38-466), diopside alumina (Da), Ca(Mg, Fe, Al) (Si, Al)₂O₆ (PDF#38-0466), augite(A) (Ca_{0.61}Mg_{0.76}Fe_{0.49}(SiO₃)₂, (PDF #76-0544) and hematite(H), Fe₂O₃ (PDF#03-0812) as mineral phases. Comparing the diffractograms of the aluminosilicate source (Pz) to that of eco-adsorbent without blowing agent (GP₀), it is observed that all the original peaks are present conforming the low dissolution mentioned at the FTIR section. There is no noticeable shift of the amorphous hump located between 20° and 35° indicating the low transformation of the aluminosilicate phases to geopolymer networks. Observing also the diffractograms of the eco-adsorbents obtained without and with addition of hydrogen peroxide (GP₀ and GP₁), it is noticed

the disappearances of the peaks at 32° , 36° and 63° . This fact reveals a probable dissolution of diopside alumina and diopside sodian minerals in hydrogen peroxide medium.

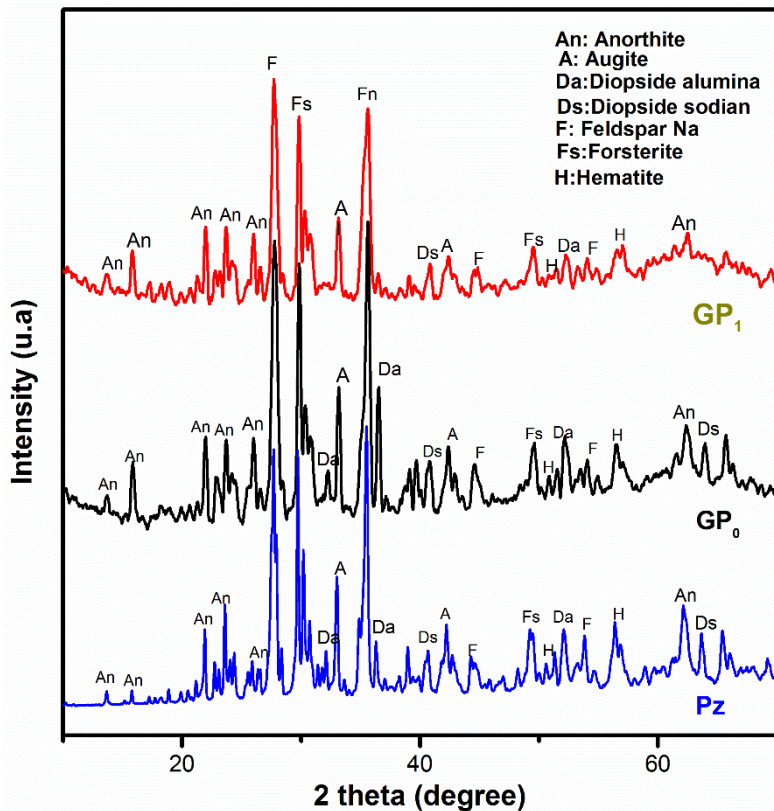


Figure 4: XRD patterns of precursor and GP₀ and GP₁ geopolymer

3.5 Scanning electron microscopy and Energy Dispersive X-ray analysis (SEM/EDX)

Figure 5 shows the micrographs of the Pz, GP₀ and GP₁ materials associated with their elemental compositions (Table 3). The Figure 5a shows that the pozzolan is mainly made of crystalline phases and the EDX analysis reveals that these phases are aluminosilicate minerals, corresponding to those mentioned in the XRD section. Comparing the microstructural of Pz to that of GP₀ material (Figure 5b), the observed densification of the microstructure of GP₀ material due to polymerization/polycondensation of aluminosilicate phases to geopolymer networks. The micrograph (figure 5c) presents the capillary pores dispersed on the microstructure of geopolymer network. This fact discloses that the blowing agent affect the structure and the microstructure of geosorbent. The elemental composition of both materials confirms that silicate, aluminate and ferrate phases participate to the geopolymerization and the negative charges of geopolymer networks are balanced by Na^+ , K^+ , Ca^{2+} and Mg^{2+} ions. Moreover, considering the values of Si/Fe ratios more significant than those of Si/Al (Table 3), it can be concluded that GP₀ and GP₁ geoadsorbents are made of poly (ferro- sialate-siloxo)

chains. It should also be noted that the presence of cracks and capillary pores on the surface of the geopolymers GP₀ (Figure 5b) and GP₁ (Figure 5c) will constitute the access routes of the adsorbates to active sites of the framework during the adsorption process.

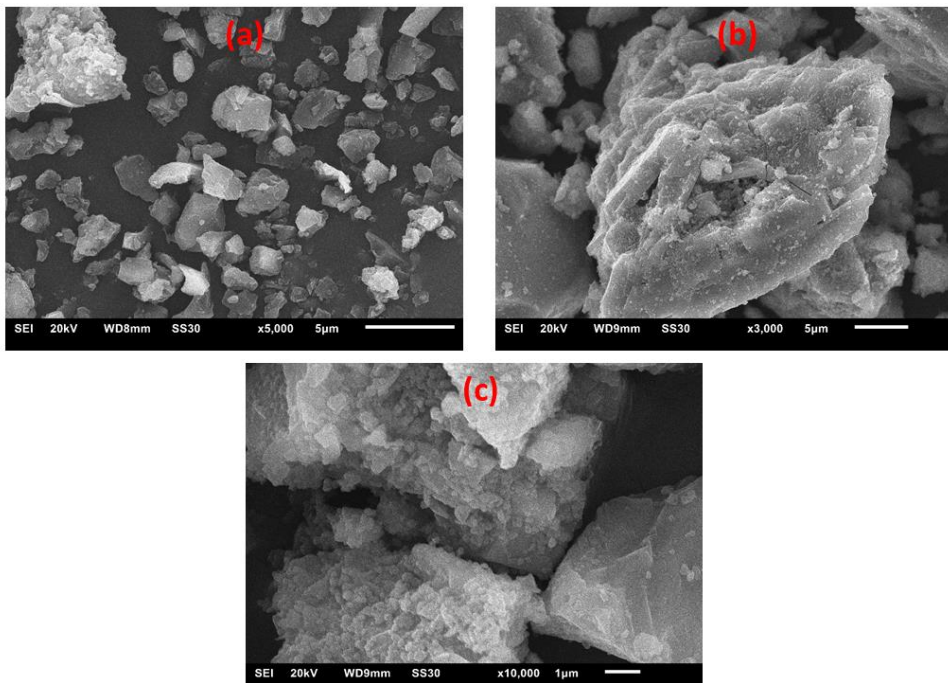


Figure 5: Scanning electron Microscopy of Pz (a), GP₀ (b) and GP₁ (c)

Table 3: EDX analysis of the Pz, GP₀ and GP₁ materials

Element	Si	Al	Fe	Ca	Mg	Na	K	O	Si/Al	Si/Fe
Material	Pz (a)									
%Element	15.11	5.80	3.12	2.39	1.63	1.46	0.38	43.71	2.60	4.84
Material	GP ₀ (b)									
%Element	15.91	6.98	5.58	6.47	2.93	2.82	0.52	45.17	2.27	2.85
Material	GP ₁ (c)									
%Element	8.77	4.26	2.77	2.68	1.86	1.66	0.25	26.18	2.06	3.16

3.6 Influence of pH

Figure 6 represents the influence of pH on the adsorption capacities of MB generally revealed that the fixation of MB is unfavorable in acidic medium on the two eco-adsorbents due the electrostatic repulsion between the MB molecules and positively charged surfaces of these materials. In addition to this repulsion at pH below 5, an increased competition between MB

cations and hydrogen ions (H^+) for the active sites of the GP_0 compared to GP_1 is implied. In contrast, in a basic medium (at pH above 7.5), the GP_0 and GP_1 surfaces became more negative and the uptake of MB cations increased due to electrostatic attractions. The increase in negatively charged adsorption sites is attributed to deprotonation of the silanols ($SiO-H$) or aluminol ($AlO-H$) groups. This is consistent with the reports by Marouane and co-workers reported for MB sequestration by a metakaolin-based geopolymers [13].

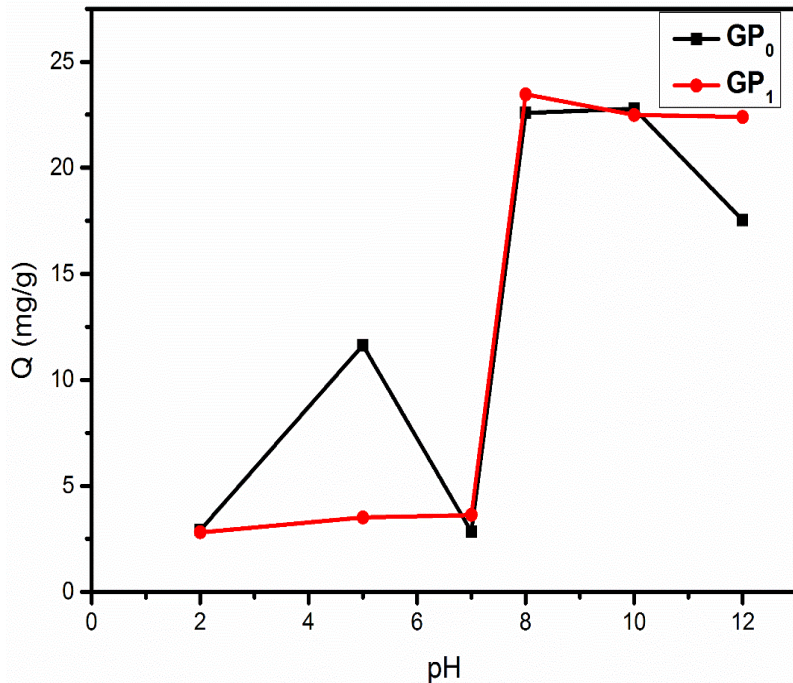


Figure 6: Influence of pH on the adsorption capacity of the different geopolymers.

3.7 Effect of adsorbent dose

Figure 7 shows that a mass of 0.2 g of geopolymers (GP_0 and GP_1) is capable to sequester at most 97.79% and 99.39% of the initial MB in solution, respectively. Beyond this mass, the quantities of MB adsorbed decrease and with no appreciable change, indicating an agglomeration of certain adsorption sites due to excess mass [29]. It will, therefore, be useful to work with adsorbent doses less than or equal to 0.2 g to avoid inefficient overdosing.

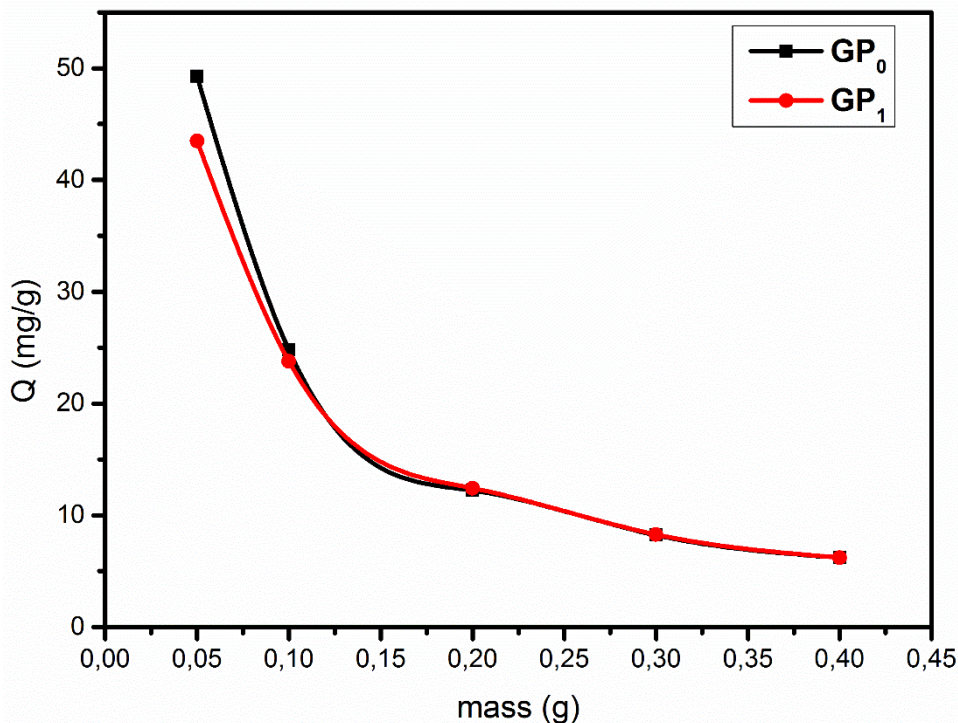


Figure 7: Influence of Adsorbent Dose

3.8 Contact time

Figure 8 represents the influence of contact time on the MB uptake by the GP_0 and GP_1 . At the very beginning of the adsorption process, a rapid increase of the adsorbed quantities is observed. This process stabilizes after 10 minutes with the appearance of an equilibrium stage for both materials. Beyond 10 min a desorption phenomenon is observed which extends from the 10th to the 20th minute for the geopolymer GP_1 and from the 10th to the 30th minute for the geopolymer GP_0 where this phenomenon is very pronounced. The adsorption process is considered to have reached the pseudo-equilibrium state after 50 minutes for the GP_0 material and 30 minutes for the GP_1 material with adsorbed quantities of MB of 22.860 mg/g and 24.470 mg/g, respectively. This kinetics can be explained by the fact that at the beginning of the process, there is a rapid occupation of the vacant adsorption sites by the MB molecules. As for the desorption phenomenon, it is due to the size of MB molecules (14.47 Å) [30] which is much smaller than the pore diameters of the GP_0 and GP_1 and allows detachment of weakly adsorbed molecules.

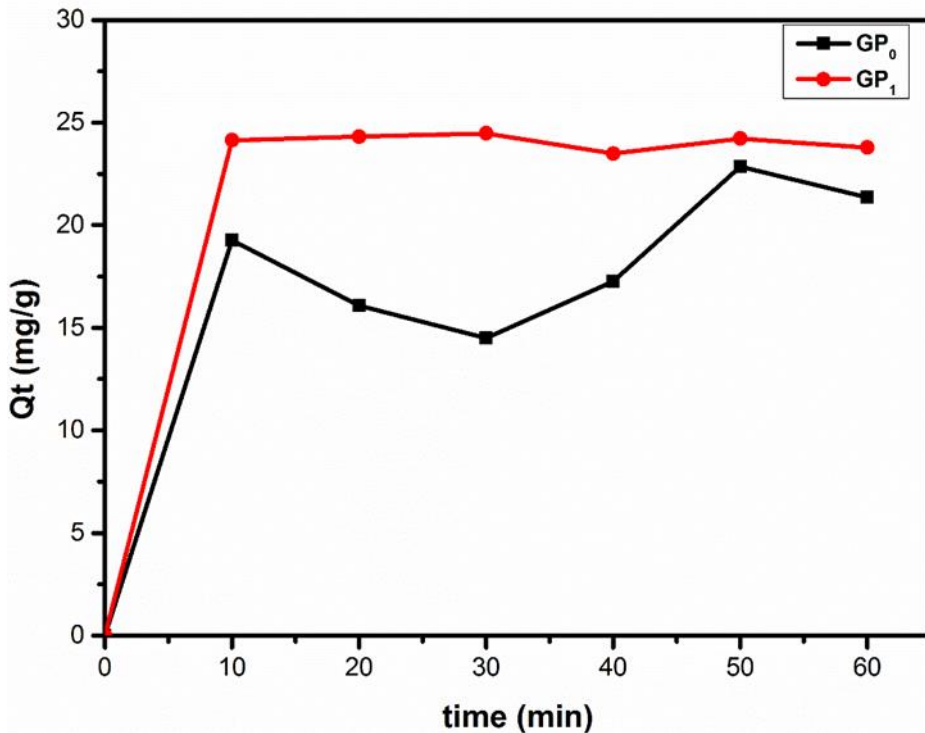


Figure 8: Effect of the MB contact time on the adsorption capacities of the different geopolymers

3.9 Kinetic study

In order to minimize errors due to linear regression as discussed in the works of Shikuku al. [31], and Chuncai al. [32], the non-linear regression method for the pseudo-first order, pseudo-second order and vermeulen kinetic models was applied to the experimental data to determine the best-fitting model, adsorption rate and predict the mechanism controlling the adsorption kinetics of methylene blue onto the geopolymers.

3.9.1 Pseudo-first-order model or Lagergren model (PFO)

The general Lagergren (1898) first-order rate expression is expressed as follows:

$$\frac{dq_t}{dt} = k_1(q_e - q_t) \quad (3)$$

Where q_t (mg/g) is the adsorbed amount at time t (min), k_1 (min^{-1}) is the pseudo-first-order rate constant and q_e is the equilibrium value of q . Integration of Eq. (4) with the initial condition $q = 0$ at $t = 0$ gives

$$q = q_e \left(1 - e^{-k_1 t}\right) \quad (4)$$

The initial value for k_1 may be obtained by using the half adsorption time $t_{1/2}$ (defined as the time when $q_t = q_e/2$) estimated from the kinetic data and the following relationship for the PFO

Model.

$$K_1 = \frac{\ln 2}{t_{1/2}} \quad (5)$$

$$S_{rate} = K_1 q_e \quad (6)$$

Where S_{rate} ($\text{mg.g}^{-1}.\text{min}^{-1}$) is the initial adsorption rate.

3.9.2 pseudo-second-order (PSO)

McKay and Ho (1998) presented a model to characterize the kinetics of adsorption taking into account both cases of a rapid fixation of solutes at the most reactive sites and that of a slow fixation at the weak sites energies. The rate law is written as follows:

$$\frac{dq_t}{dt} = K_2 (q_e - q_t)^2 \quad (7)$$

The integrated form can be written as

$$q = \frac{K_2 q_e^2 t}{1 + K_2 q_e t} \quad (8)$$

An initial trial value for $K_2 q_e$ may be obtained by using the following relationship for the PSO model

$$K_2 q_e = \frac{1}{t_{1/2}} \quad \text{With} \quad S_{rate} = k_2 q_e^2 \quad (9)$$

where: K_2 ($\text{g}.\text{mg}^{-1}.\text{min}^{-1}$) is the pseudo-second-order rate constant and S_{rate} ($\text{mg.g}^{-1}.\text{min}^{-1}$) is the initial adsorption rate.

3.9.3 Vermeulen model

The Vermeulen model is based on the assumption that intraparticle diffusion is the controlling mechanism of adsorption. It is also known as the Urano model or the Dumwald–Wagner model [33]. The integrated Vermeulen model can be expressed as

$$q = q_e (1 - e^{-Bt}) \quad (10)$$

An initial trial value for intraparticle diffusion constant B (min^{-1}) may be obtained by using the relationship for the Vermeulen model

$$B = \frac{\ln(4/3)}{t_{1/2}} \quad (11)$$

Table 4 presents the parameters of the pseudo first-order, pseudo second order and intra-particle diffusion kinetic models. The pseudo-second order kinetic model (Figure 9) is the best to describe the MB adsorption mechanism on geopolymers GP₀ and GP₁ compared to the other

kinetics models studied with the coefficients of determination (R^2) values are closest to unity and the model-predicted quantities of MB adsorbed (19.521 mg/g and 24.073 mg/g, respectively) are very close to those obtained experimentally (22.858 mg/g and 24.473 mg/g, respectively). The adsorption mechanism is thought to take place in the following sequence: diffusion of the solute molecule towards the surface of the geopolymers, followed by displacement of the solute towards the interior of the pores and finally fixation of the solute towards the active sites inside the pores [34]. It also reflects the existence of interactions between the surface of the adsorbent and the adsorbate, suggesting a multi-mechanistic chemisorption mechanism [35]. Noteworthy, the initial adsorption rate for MB uptake by GP₁ was higher than GP₀. The fast adsorption of MB GP₁ is attributed to the larger surface area of GP₁ than GP₀ resulting to easier and faster access to the binding sites in GP₁. This reveals that the use of hydrogen peroxide as a blowing porogen during the synthesis modifies the textural properties (porosity and the specific surface area) but does not increase the identity of the binding sites as shown by the FTIR results.

Table 4: Parameters obtained from kinetic models

Models	Parameters	GP ₀	GP ₁
Pseudo first order	K ₁ (min ⁻¹)	1.996	2.523
	q _e (cal) (mg g ⁻¹)	18.550	24.069
	q _e (exp) (mg g ⁻¹)	22.858	24.473
	t _{1/2} (min)	0.347	0.275
	Srate (mg.g ⁻¹ .min ⁻¹)	37.030	60.726
	R ²	0.852	0.998
Pseudo second order	K ₂ (g mg ⁻¹ min ⁻¹)	0.039	9.999
	q _e (cal) (mg g ⁻¹)	19.521	24.073
	q _e (exp) (mg g ⁻¹)	22.858	24.473
	t _{1/2} (min)	1.316	0.004
	Srate (mg.g ⁻¹ .min ⁻¹)	14.837	5794.644
	R ²	0.858	0.998

Vermeulen	B (min^{-1})	3.216	3.216
	$q_e(\text{cal}) (\text{mg g}^{-1})$	18.551	24.069
	$q_e(\text{exp}) (\text{mg g}^{-1})$	22.858	24.473
	$t_{1/2} (\text{min})$	0.0894	0.089
	R^2	0.852	0.998

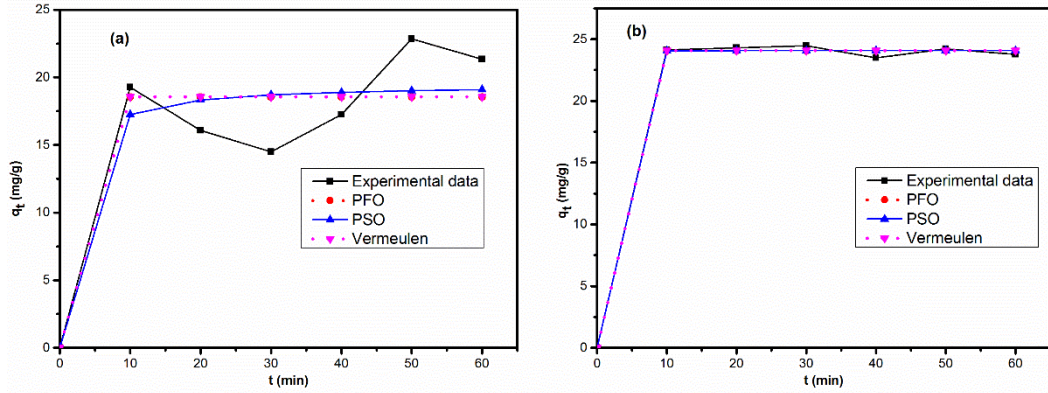


Figure-9: PFO, PSO and Vermeulen models applied to the experimental kinetic data for the adsorption of MB on different geopolymers ((a) GP₀ and (b) GP₁)

3.10 Influence of initial concentration

From Figure 10, the quantities adsorbed in MB increase linearly with the initial MB concentrations of 4.71-21.35mg/g and 4.89-23.78mg/g for GP₀ and GP₁ materials, respectively. This observation implies that an increase in MB concentration increases the diffusion and fixation of the solute molecules within the pores of these geopolymers.

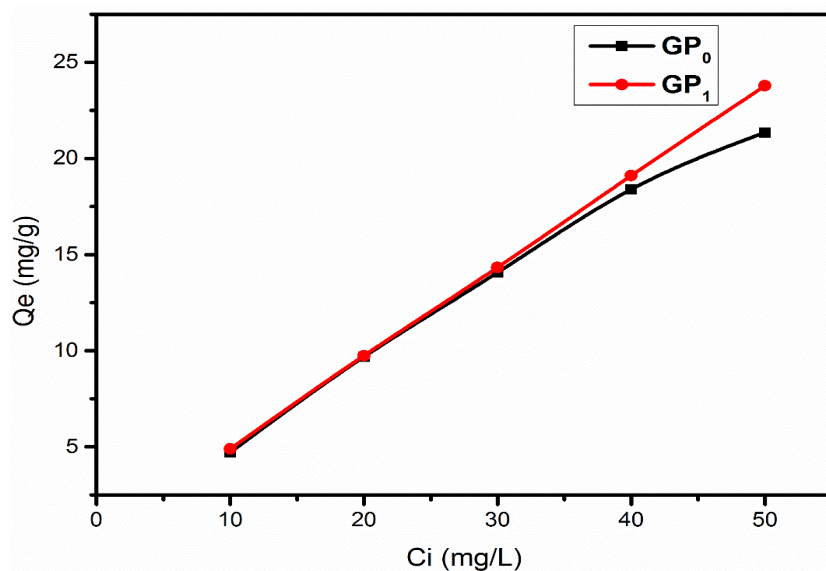


Figure 10: effect of initial concentration

3.11 Isotherms adsorption

Experimental equilibrium data were analyzed using five theoretical non-linear adsorption isotherms (Langmuir, Freundlich, Temkin, Dubinin-Radushkevich-Kaganer and Sips) to determine the model that best predicts the adsorption data and therefore best describes the adsorption mechanism of methylene blue on these eco-adsorbents.

3.11.1 Langmuir Isotherm

Langmuir isotherm (Langmuir, 1916) suggests a one-one association between adsorbate and adsorbent resulting in the formation of a monolayer. The adsorption data are validated by determining the uptake capacity (q_e) and adsorption parameters using Eq. (12) where q_e (mg/g) is the amount adsorbed at equilibrium and C_e (mg/L) is the equilibrium concentration.

$$q_e = \frac{Q_m K_L C_e}{1 + K_L C_e} \quad (12)$$

Where q_e is the amount of MB adsorbed at equilibrium (mg g⁻¹), C_e is the MB concentration in the aqueous phase at equilibrium (mg L⁻¹), Q_m is the Langmuir maximum adsorption capacity (mg g⁻¹) and K_L is the Langmuir constant (L g⁻¹). The dimensionless separation factor, R_L , was calculated using Eq. (13) [36]. The R_L value indicates whether the adsorption is favorable ($0 < R_L < 1$), unfavorable ($R_L > 1$), linear ($R_L = 1$), or irreversible ($R_L = 0$) [34].

$$R_L = \frac{1}{1 + K_L C_0} \quad (13)$$

3.11.2 Freundlich Isotherm

The Freundlich isotherm model (Freundlich, 1906) is an empirical equation that is applied to multilayer adsorption. This model assumes that the surface of the adsorbent is heterogeneous and active sites and their energies distribute exponentially. The Freundlich isotherm is expressed as Eq. (14):

$$q_e = K_F C_e^{\frac{1}{n}} \quad (14)$$

Where K_F is the Freundlich constant (L g⁻¹) and the parameter n is a dimensionless constant.

3.11.3 Dubinin-Radushkevich Kaganer isotherm

The Dubinin-Radushkevich-Kaganer (D-R-K) isotherm (Eq.15) is applied to the adsorption process onto a microporous adsorbent. It estimates the energy of adsorption and distinguishes between physisorption or chemisorption nature of adsorption onto homogeneous and heterogeneous surfaces [36].

$$Q_e = Q_m \exp(-\beta \xi^2) \quad (15)$$

Where Q_e is the amount of adsorbate adsorbed per unit dosage of the adsorbent at equilibrium (mol/g) and Q_m is the theoretical monolayer saturation capacity (mol/g) [37]. The Polanyi potential (ξ) is expressed as

$$\xi = RT \ln\left(1 + \frac{1}{c_e}\right) \quad (16)$$

The mean sorption energy E_a (kJ/mol) of the adsorbate (Eq.17) identifies the physical and chemical interactions between the adsorbate and adsorbent during the adsorption process.

$$E_a = \frac{1}{\sqrt{2\beta}} \quad (17)$$

3.11.4 Temkin isotherm

The Temkin isotherm model contains a factor that explicitly takes into account the adsorbent–adsorbate interactions. The heat of adsorption of all the molecules in the layer would decrease linearly with coverage due to adsorbent–adsorbate interactions. The adsorption is characterized by a uniform distribution of binding energies, up to some maximum binding energy. The Temkin adsorption isotherm expression is shown in Eq. (18) [38].

$$q_e = B_T \ln(A_T C_e) \quad (18)$$

Where $B_T = RT/b_T$, b (J/mol) is the Temkin constant relating to the heat of sorption; A (L/g) is the Temkin isotherm constant. R is the universal gas constant (8.314 J/mol.K), and T (K) the absolute temperature.

3.11.5 Sips isotherm

By identifying the problem of continuing increase in the adsorbed amount with an increase in concentration in the Freundlich equation, Sips proposed an equation that combines the Freundlich and Langmuir isotherms. This produces an expression that exhibits a finite limit at sufficiently high concentration. This model is valid for predicting the heterogeneous adsorption systems and localized adsorption without adsorbate-adsorbate interactions. The Sips isotherm model is given by Eq. (19):

$$Q_e = \frac{Q_{ms} a_s C_e^{B_s}}{1 + a_s C_e^{B_s}} \quad (19)$$

Where Q_{ms} , a_s and B_s are the isotherm constants. The constant B_s is the heterogeneity index.

The assessment of the validity of the results in Table 5 was based on the values of the coefficient of determination, R^2 . The equilibrium data was described by the models in the order Sips >Temkin >Langmuir > D-K-R >Freundlich model for the GP₀ and Freundlich > Sips >Langmuir > Temkin > D-K-R model for the material GP₁.

The Freundlich isotherm is appropriate to describe the adsorption mechanism of MB on the geopolymer GP₁ and the value of the Freundlich parameter n lower than 1, implies that the adsorption sites of this geopolymer are heterogeneous, consequently the adsorption is carried out in multilayer and the isotherm is linear of H type (Figure 12b) [39].

The Sips isotherm, was the most appropriate to describe the adsorption of MB on geopolymer GP₀. The heterogeneity factor (B_s) of 1.14893 greater than unity, indicates a heterogeneity of the system resulting from the interaction adsorbent-adsorbate [40]. The adsorption capacities can be estimated using the sips isotherm model, therefore it follows that the adsorption capacity of MB are high on the GP₁ (366.196 mg/g) than GP₀ (24.440 mg/g). This could be justified simply by the high pore volume and specific surface area that GP₁ has compared to GP₀ (Table 2). The high adsorption capacity of MB GP₁ material (15 times higher than that of GP₀ material) is also justified by the various phenomena possibly taking place within the multiple pores (Figure 11) such as:

- Electrostatic interactions between the negative sites of geopolymers and positives sites of MB.
- Ions exchange between the MB cations and counter ions (Na⁺, K⁺, Ca²⁺and Mg²⁺).
- Formation of dative bonds between the nitrogen doublets of MB molecules and the empty quantum cells of the GP₁ material.

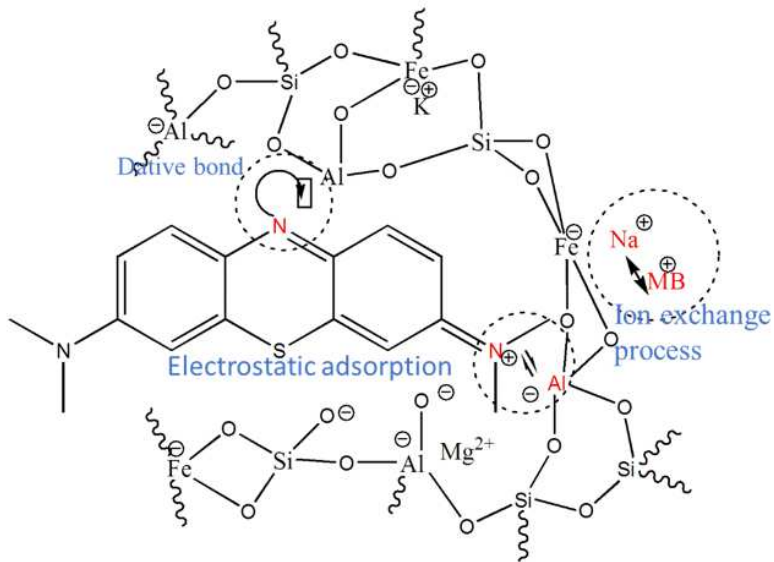


Figure 11: Interaction mechanisms in the GP1-MB system.

The D-R -K model shows that the adsorption energy of the two synthetic materials is less than 8 kJ/mol which suggests that physisorption is the dominant adsorption mechanism [41].

Table 5: Parameters obtained from adsorption isotherms

Isotherms	Parameter	GP ₀	GP ₁
Langmuir	Q _{max} (mg/g)	23.897	30.102
	K _L (L/mg)	0.915	0.838
	R _L	0.021	0.023
	R ²	0.917	0.981
Freundlich	K _F (mg/g) (L/mg) ⁻¹	10.183	13.242
	1/n	0.403	0.627
	R ²	0.884	0.982
D – R – K	Q _{max} (mg/g)	20.181	22.076
	E _a (kJ/mol)	1.036	1.374
Temkin	R ²	0.907	0.873
	A (L/g)	5.692	8.215
	ΔQ (kJ/mol)	5.953	7.152
	R ²	0.933	0.936

	Q_{\max} (mg/g)	24.440	366.196
Sips	a_s	0.730	0.038
	B_s	1.1489	0.652
	R^2	0.941	0.981

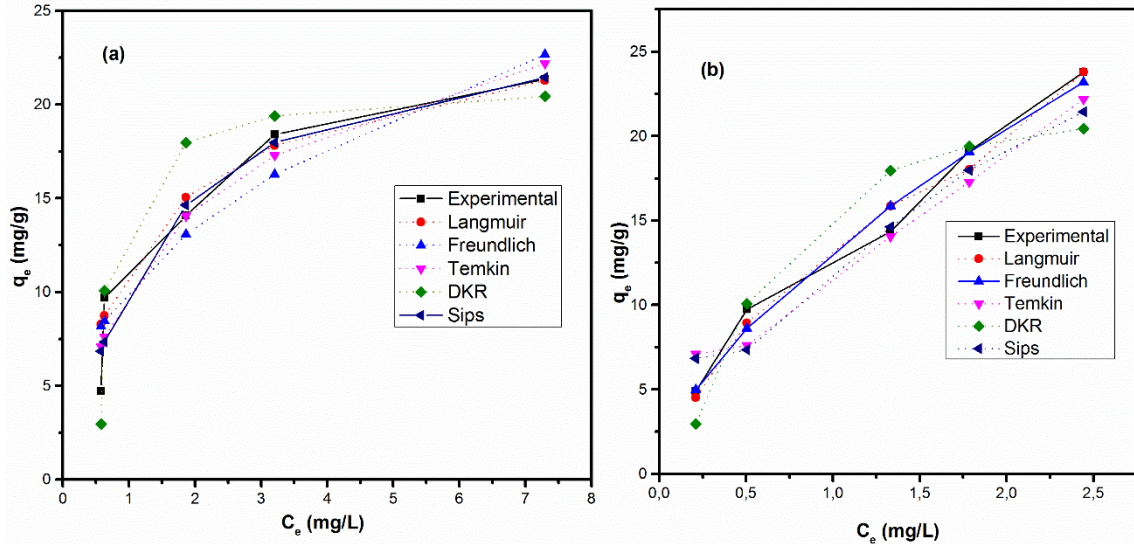


Figure 12: Adsorption isotherm plots for MB onto (a) GP₀ and (b) GP₁ materials

3.12. Adsorption thermodynamics

The effect of temperature and adsorption thermodynamics functions were evaluated in the temperature range 309-339 K. The thermodynamic functions, enthalpy change (ΔH), Gibb's free energy (ΔG), and entropy (ΔS) were calculated using equations 20-23 and the calculated parameters for MB uptake are listed in Table 6.

$$\Delta G = -RT \ln K_c \quad (20)$$

$$K_d = \frac{C_{ads}}{C_e} \quad (21)$$

$$K_c = 1000 K_d \quad (22)$$

$$\ln K_c = \frac{\Delta S}{R} - \frac{\Delta H}{R} \frac{1}{T} \quad (23)$$

Where K_c is the equilibrium constant (dimensionless), C_e is the residual dye concentration in the aqueous phase at equilibrium (mg L⁻¹) and C_{ads} is the dye concentration in the adsorbent at

equilibrium (mg g^{-1}), K_d is the distribution coefficient (L/g) and the density of water is 1000 g/L . R is the gas constant ($8.314 \text{ J mol}^{-1}\text{K}^{-1}$) and T is the temperature (K).

The positive enthalpy (ΔH) values confirm that adsorption of the MB on the eco-adsorbents is an endothermic reaction. The negative ΔG values, reveal the feasibility and spontaneity of MB removal on both geopolymers. The decrease in the magnitude of ΔG with rise in temperature imply the reaction becomes more and more spontaneous and the amount adsorbed increases with increased temperature consistent with an endothermic process (Figure 13). The relatively low ΔG values correspond to a physical process. The positive values of entropy denote that the approach and distribution of MB molecules through the pores of GP_0 and GP_1 materials is disordered. In addition, the ΔH values below 40 kJ mol^{-1} indicate that the sorption of MB on these eco-adsorbents entails a physisorption mechanism, consistent with the prediction from D-K-R model [42].

Table 6: Thermodynamic functions for MB uptake by GP_0 and GP_1

Adsorbent	Temp.	ΔG	ΔH	ΔS
	(K)	(kJ mol ⁻¹)	(kJ mol ⁻¹)	(kJ mol ⁻¹)
GP₀	309	-16.02		
	319	-16.66		
	329	-17.92	32.20	0.15
	339	-20.84		
GP₁	309	-17.49		
	319	-18.91		
	329	-19.81	20.62	
	339	-21.31		0.12

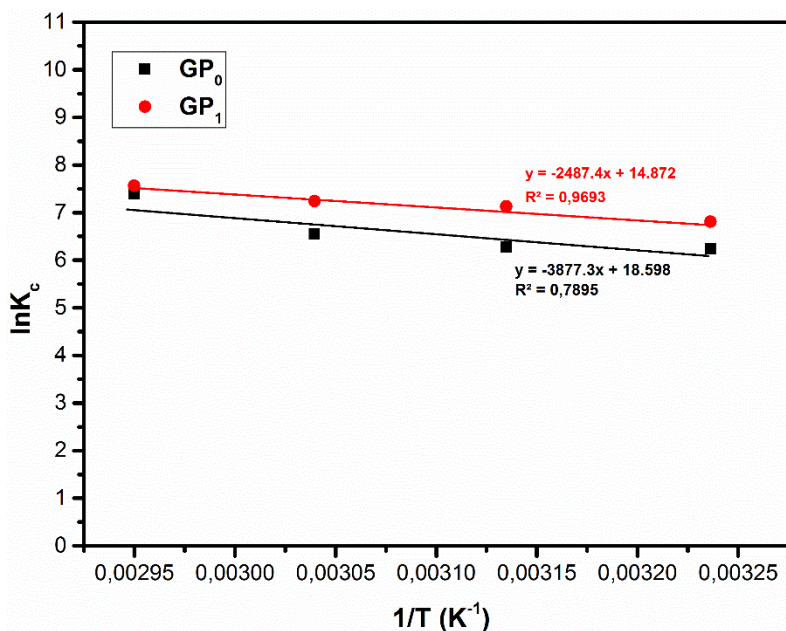


Figure 13: Isotherm plot of van't Hoff.

4. Conclusion

The development the pozzolan-based eco-adsorbents was done by geopolymmerization using hydrogen peroxide as a blowing agent with mass ratios 0 and 1%, labeled GP₀ and GP₁ respectively, in order to modify the textural properties and to evaluate their performance in removing the basic dye methylene blue in aqueous solution. The physico-chemical characteristics revealed that the incorporation of 1% blowing agent increased the specific surface area from 4.344 to 5.610 m²/g. The increase in surface area resulted to an increase in adsorption capacity by 15 orders of magnitude from 24.4 to 366.2 mg/g for GP₀ and GP₁, respectively. The adsorption rates of methylene blue on the two eco-adsorbents were best described by the pseudo-second order kinetic model. The adsorption equilibrium data were best described by the Sips and Freundlich isotherms models for GP₀ and GP₁, respectively. Thermodynamically, it was determined that the adsorption of methylene blue onto eco-adsorbents is a physical and endothermic process. The results show that incorporation of hydrogen peroxide into pozzolan-based geopolymers increases their adsorption capacity for methylene blue dye stupendously relative under the experimental conditions reported.

Acknowledgements

We thank Institute of Inorganic chemistry and structural in Dusseldorf (Germany) for the characterization of raw materials and geopolymers samples.

Author Contributions

David Dina, Sylvain Tome: Validation, Methodology, Writing - review & editing, Visualization, original draft. Dzoujo T. Hermann, Jean T. Tchuigwa: Conceptualization, Methodology, Investigation, writing - original draft, resources. Victor O. Shikuku: Validation, Writing - review & editing. Alex Spieß: Validation, Writing - review & editing, Marie-Annie Etoh: Writing - review & editing, Visualization. David Dina, Marie-Annie Etoh, Christoph Janiak: Resources, Supervision

Funding

The authors of manuscript did not receive any funding and grants for this work.

Availability of data and materials

All data generated or analyzed during this study are included in this article.

Compliance with ethical standards

Conflict of interest

The authors declare that they have no conflict of interest.

Consent to participate

Not Applicable

Consent for publication

Not Applicable

References

1. Fatima Zohra Choumane, (2015) Elimination des métaux lourds et pesticides en solution aqueuse par des matrices argileuses, Thèse de Doctorat, Chimie de l'environnement.
2. Taylor, Publisher, Mark A. Brown, and Stephen C. De Vito. (2009) “Critical Reviews in Environmental Science and Technology Predicting Azo Dye Toxicity Predicting Azo Dye Toxicity.” (June 2013):37–41.
3. Ghosh, Dipa, and Krishna G. Bhattacharyya. (2002) “Adsorption of Methylene Blue on Kaolinite.” 20:295–300.
4. ALVARES A.B.C., C. DLAPER et S.A. PARSONS. (2013) Partial oxidation by ozone to remove recalcitrance from wastewaters – a review. Environ. Technol., 22, 409-427
5. Badawi, M. A., N. A. Negm, M. T. H. Abou Kana, H. H. Hefni, and M. M. Abdel Moneem.(2017). “Adsorption of Aluminum and Lead from Wastewater by Chitosan-Tannic Acid Modified Biopolymers: Isotherms, Kinetics, Thermodynamics and Process Mechanism.” *International Journal of Biological Macromolecules*.doi: 10.1016/j.ijbiomac.2017.03.003.

6. Sharma, P., Kaur, H., Sharma, M., & Sahore, V. (2011) *A review on applicability of naturally available adsorbents for the removal of hazardous dyes from aqueous waste* 151–195. <https://doi.org/10.1007/s10661-011-1914-0>
7. US Department of the interior and US Geological Survey (2010). Minerals yearbook, metals and minerals, vol 1. Government Printing Office, Washington DC.
8. Billong N, Melo UC, Njopwouo N, Louvet F, Bonnet JP. (2013) Physicochemical characteristics of Some Cameroonian pozzolans for use in sustainable cement like materials. *Mater Sci Appl* 4:14–21.
9. Wamba, A. G. N., Lima, E. C., Ndi, S. K., Thue, P. S., Kayem, J. G., Rodembusch, F. S., dos Reis, G. S., & de Alencar, W. S. (2017) Synthesis of grafted natural pozzolan with 3 aminopropyltriethoxysilane: preparation, characterization, and application for removal of Brilliant Green 1 and Reactive Black 5 from aqueous solutions. *Environmental Science and Pollution Research*, 24(27), 21807–21820. .
10. Kofa, G. P., S. NdiKoungou, G. J. Kayem, and R. Kamga . (2015) “Adsorption of Arsenic by Natural Pozzolan in a Fixed Bed: Determination of Operating Conditions and Modeling.” *Journal of Water Process Engineering* 6:166–73. doi: 10.1016/j.jwpe.2015.04.006.
11. Gaston Fumba, Jean Serge Essomba, Guy Merlin Tagne, Julius Ndi Nsami, Placide Désiré Bélibi Bélibi and Joseph Ketcha Mbadiwa. (2014) Equilibrium and Kinetic Adsorption Studies of Methyl Orange from Aqueous Solutions Using Kaolinite, Metakaolinite and Activated Geopolymer as Low Cost Adsorbents, *Journal of Academia and Industrial Research (JAIR)* Volume 3, 156–163.
12. Novais, R.M., Ascensão, G., Tobaldi, D.M., Seabra, M.P., Labrincha, J.A. (2018) Biomass Fly ash geopolymer monoliths for effective methylene blue removal from wastewaters. *J. Clean. Prod.*, 171, 783794.
13. Marouane, E., Saliha, A., Mohammed, E., Taibi, M. (2019) Preparation, Characterization, and Application of Metakaolin-Based Geopolymer for Removal of Methylene Blue from Aqueous Solution. *J. Chem.* <https://doi.org/10.1155/2019/4212901>.
14. Bai, Chengying, and Paolo Colombo. (2018) “Processing, Properties and Applications of Highly Porous Geopolymers: A Review.” *Ceramics International* 44(14):16103–18. doi:10.1016/j.ceramint.2018.05.219.

15. Singhal, Aditi; Gangwar, Bhanu P.; Gayathry, J.M. (2017). CTAB modified large surface area nanoporous geopolymers with high adsorption capacity for copper ion removal. *Applied Clay Science*, 150(), 106–114. doi:10.1016/j.clay.2017.09.013
16. Sarkar, Chayan; Basu, Jayanta Kumar; Samanta, Amar Nath (2018). Experimental and kinetic study of fluoride adsorption by Ni and Zn modified LD slag based Geopolymer. *Chemical Engineering Research and Design*, S0263876218306221–. doi:10.1016/j.cherd.2018.12.006
17. Runtti, Hanna; Luukkonen, Tero; Niskanen, Mikko; Tuomikoski, Sari; Kangas, Teija; Tynjälä, Pekka; Tolonen, Emma-Tuulia; Sarkkinen, Minna; Kemppainen, Kimmo; Rämö, Jaakko; Lassi, Ulla (2016). Sulphate removal over barium-modified blast-furnace-slag geopolymers. *Journal of Hazardous Materials*, S0304389416305568–. doi:10.1016/j.jhazmat.2016.06.001
18. M. Sido-Pabyam, M. Gueye, J. Blin, E. Some (2009). Valorisation de résidus de Biomasse en Charbons actifs – Tests d'efficacité sur des bactéries et dérivés de pesticides. *Revue Sud Sciences et Technologies*, 17, 65-73.
19. Karadag, Dogan (2007). “Modeling the Mechanism, Equilibrium and Kinetics for the Adsorption of Acid Orange 8 onto Surfactant-Modified Clinoptilolite : The Application of Nonlinear Regression Analysis.” 74. doi: 10.1016/j.dyepig.2006.04.009.
20. Davidovits, J. (2008) Geopolymer Chemistry & Applications. Geopolymer Institute, Saint-Quentin.
21. Siyal, A. A., Shamsuddin, M. R., Khan, M. I., Rabat, E., Zulfiqar, M., Man, Z., Siame, J., & Azizli, K. A. (2018) A Review on Geopolymers as Emerging Materials for the. *Journal of Environmental Management*. <https://doi.org/10.1016/j.jenvman.2018.07.046>
22. Sangwichien, C., G. L. Aranovich, and M. D. Donohue (2002). “Density Functional Theory Predictions of Adsorption Isotherms with Hysteresis Loops.” 206:313–20.
23. Khan, M. I., Min, T. K., Azizli, K., Sufian, S., Ullah, H., & Man, Z. (2015) Effective removal of methylene blue from water using phosphoric acid based geopolymers: Synthesis, characterizations and adsorption studies. *RSC Advances*, 5(75), 61410–61420. <https://doi.org/10.1039/c5ra08255b>.
24. Tahir S.S. and Naseem Rauf (2006). Removal of cationic dye from aqueous solutions by adsorption onto bentonite clay. *Chemosphere*. 63, 1842-1848 *Ceramics International*, 44(14), 16103–16118. <https://doi.org/10.1016/j.ceramint.2018.05.219>
25. Panias, Dimitrios, Ioanna P. Giannopoulou, and Theodora Perraki (2007). “Effect of

- Synthesis Parameters on the Mechanical Properties of Fly Ash-Based Geopolymers.” 301:246–54. doi: 10.1016/j.colsurfa.2006.12.064.
26. Maragkos, Ioannis, Ioanna P. Giannopoulou, and Dimitrios Panias (2009). “Synthesis of Ferronickel Slag-Based Geopolymers.” 22:196–203. doi: 10.1016/j.mineng.2008.07.003.
27. Rattanasak, Ubolluk, and Prinya Chindaprasirt (2009). “Influence of NaOH Solution on the Synthesis of Fly Ash Geopolymer.” Minerals Engineering 22(12):1073–78. doi: 10.1016/j.mineng.2009.03.022.
28. Tome, S., Etoh, M., Etame, J., & Kumar, S. (2020) Improved Reactivity of Volcanic Ash using Municipal Solid Incinerator Fly Ash for Alkali-Activated Cement Synthesis. Waste and Biomass Valorization, 11(6), 3035–3044. <https://doi.org/10.1007/s12649-019-00604-1>
29. Karim, A. B., Mounir, B., Hachkar, M., Bakasse, M., & Yaacoubi, A. (2010) Élimination du colorant basique « Bleu de Méthylène » en solution aqueuse par l’argile de Safi. Revue Des Sciences de l’eau, 23(4), 375–388 .<https://doi.org/10.7202/045099ar>
30. Dotto, G. L., J. M. N. Santos, I. L. Rodrigues, R. Rosa, F. A. Pavan, and E. C. Lima. “Adsorption of Methylene Blue by Ultrasonic Surface Modified Chitin.” *JOURNAL OF COLLOID AND INTERFACE SCIENCE* (2015). doi: 10.1016/j.jcis.2015.01.046.
31. Shikuku, V. O., Kowenje, C. O., & Kengara, F. O. (2018) Errors in Parameters Estimation Using Linearized Adsorption Isotherms : Sulfadimethoxine Adsorption onto Kaolinite Clay. 23(4), 1–6. <https://doi.org/10.9734/CSJI/2018/44087>
32. Yao, C., & Chen, T. (2019) An improved regression method for kinetics of adsorption from aqueous solutions. Journal of Water Process Engineering, 31(May), 100840. <https://doi.org/10.1016/j.jwpe.2019.100840>
33. G. McKay, M.S. Otterburn, J.A. Aga. (1985) Fuller’s earth and fired clay as adsorbents for dyestuffs, Water, Air, Soil Pollut. 24, 307–322.
34. Ofomaja, Augustine E. (2008) “Sorptive Removal of Methylene Blue from Aqueous Solution Using Palm Kernel Fibre: Effect of Fibre Dose.” 40:8–18. doi: 10.1016/j.bej.2007.11.028.
35. Mariame Conde Asseng, Hermann Tamaguelon Dzoujo, Daniel David Joh Dina, Marie Annie Etoh, Armand Ngoungue Tchakounte, and Julius Ndi Nsami (2020). “Batch Studies for the Removal of a Hazardous Azo Dye Methyl Orange from Water through Adsorption on Regenerated Activated Carbons.” Journal of Materials Science and Engineering B 10(3):109–23. doi: 10.17265/2161-6221/2020.5-6.003.

36. Itodo AU, Itodo HU. (2010) Sorption energies estimation using Dubinin Radushkevich and Temkin adsorption isotherms. *Life Sci* 7:31–39.
37. Jia, L. I. U., Wang Hong-liang, L. Ü. Chun-xin, L. I. U. Han-fei, G. U. O. Zhi-xin, and Kang Chun-li (2013). “Water Through Modified Diatomite.” 29(2007):3–6. doi: 10.1007/s40242-013-2504-1.
38. M.I. Temkin, V. Pyzhev (1940). Kinetics of ammonia synthesis on promoted iron catalyst, *Acta Physiochim. URSS* 12, 327–356.
39. Freundlich H. (1906) on adsorption in solution. *Z. Physik. Chem.*, vol. 57, pp385-471.
40. R. Sips (1948), on the structure of a catalyst surface, *J. Chem. Phys.*, 16, 490.
41. Anagho S., Tchuifon R., Ndifor-Angwafor G., Ndi J., Ketcha J., Nchare M. (2013) "Nickel adsorption from aqueous solution onto kaolinite and metakaolinite: kinetic and equilibrium studies." *International Journal of Chemistry*, 4, 1-7.
42. Shikuku V.O., and Kimosop, J. (2020) efficient removal of sulfamethoxazole onto sugarcane bagasse-derived biochar: two and three-parameter isotherms, kinetics and thermodynamics. *S. Afr. J. Chem.*, 73, 111-119.

Figures

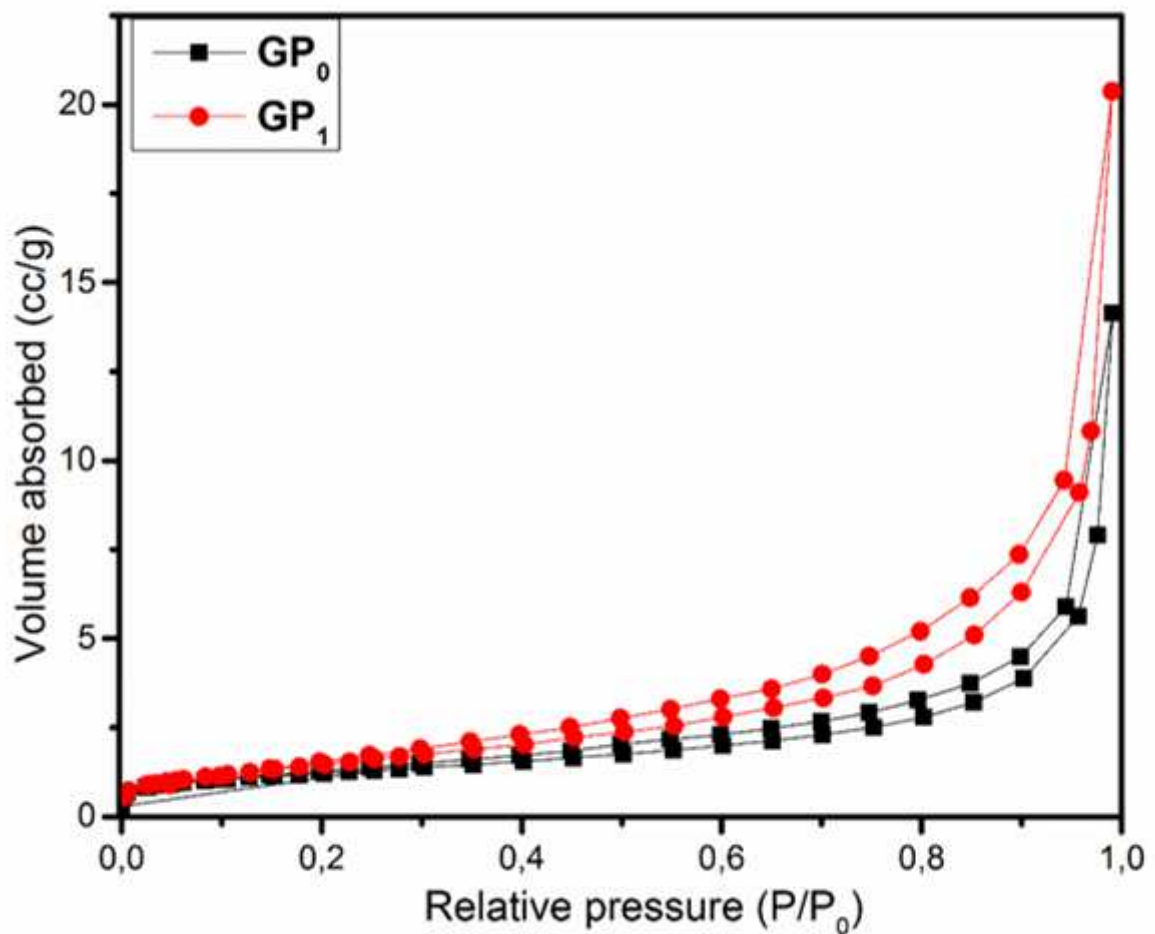


Figure 1

N₂ adsorption-desorption isotherms of eco-adsorbents materials

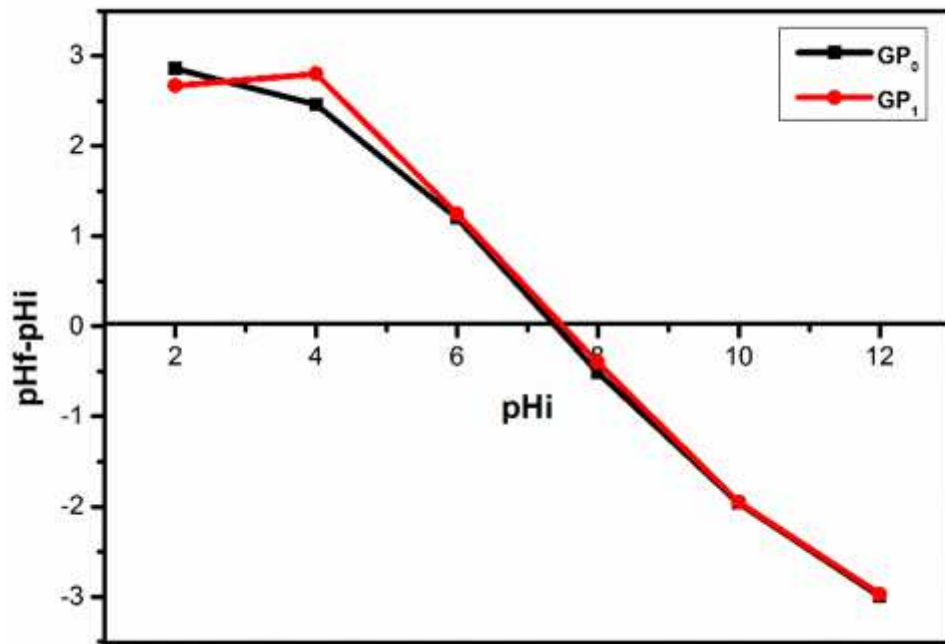


Figure 2

Point of Zero Charge of geopolymers materials.

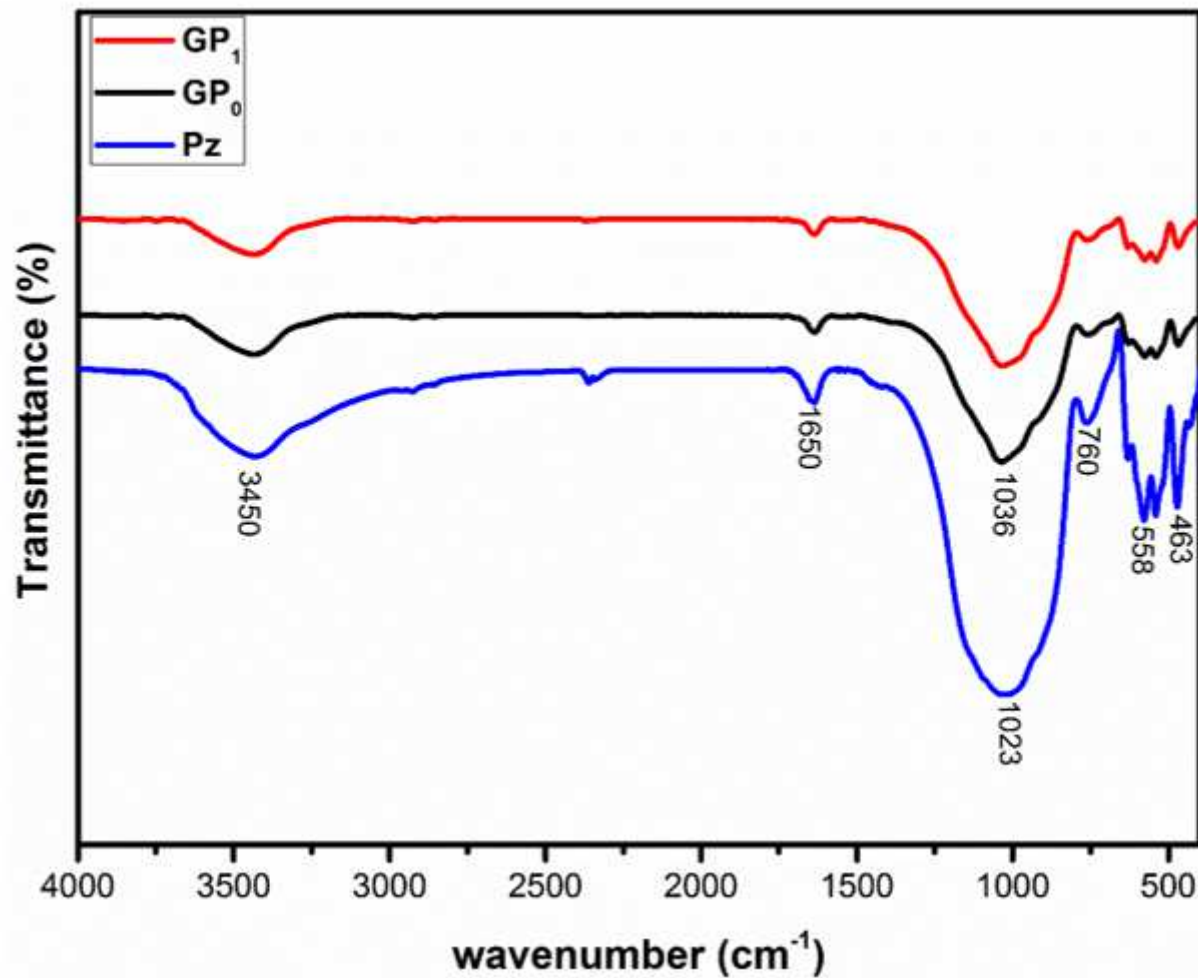


Figure 3

FTIR of the samples Pz, GP0 and GP1

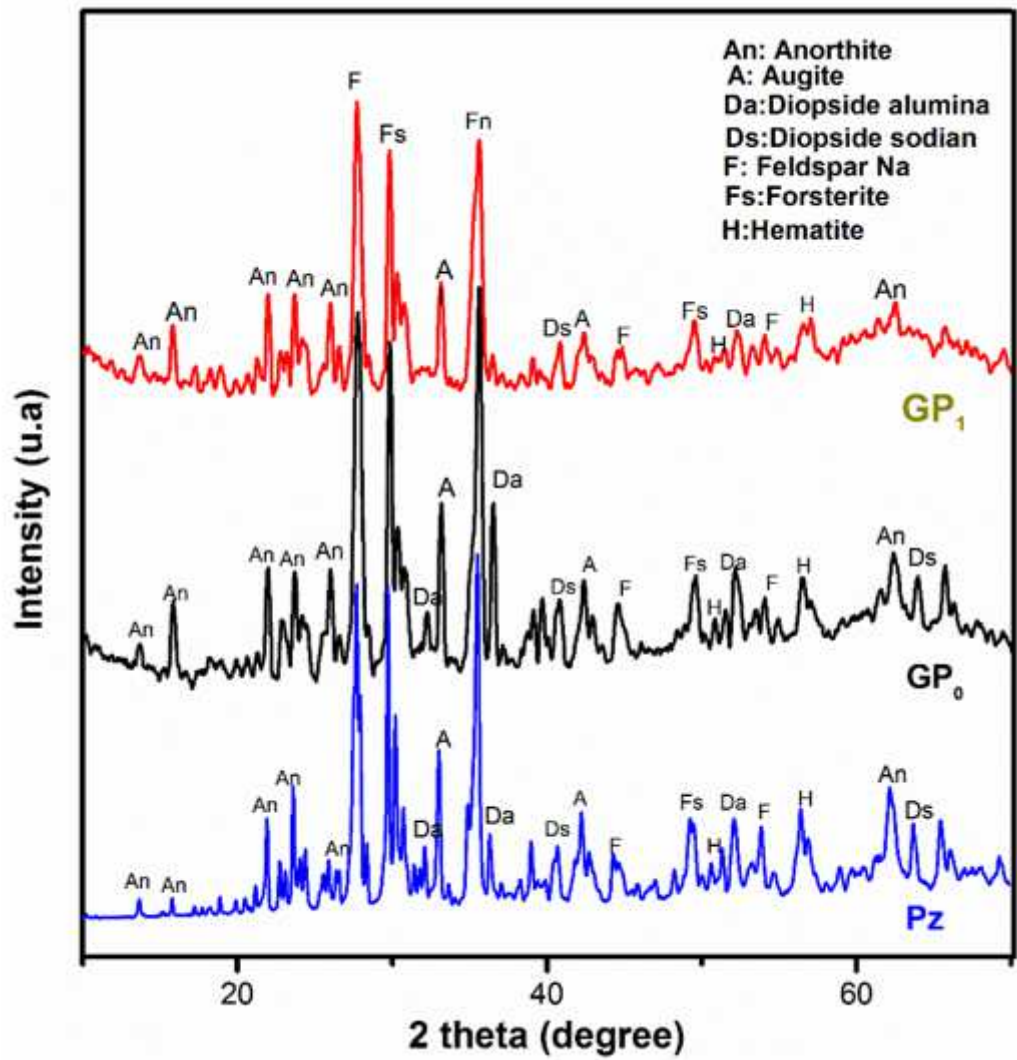


Figure 4

XRD patterns of precursor and GP0 and GP1 geopolymer

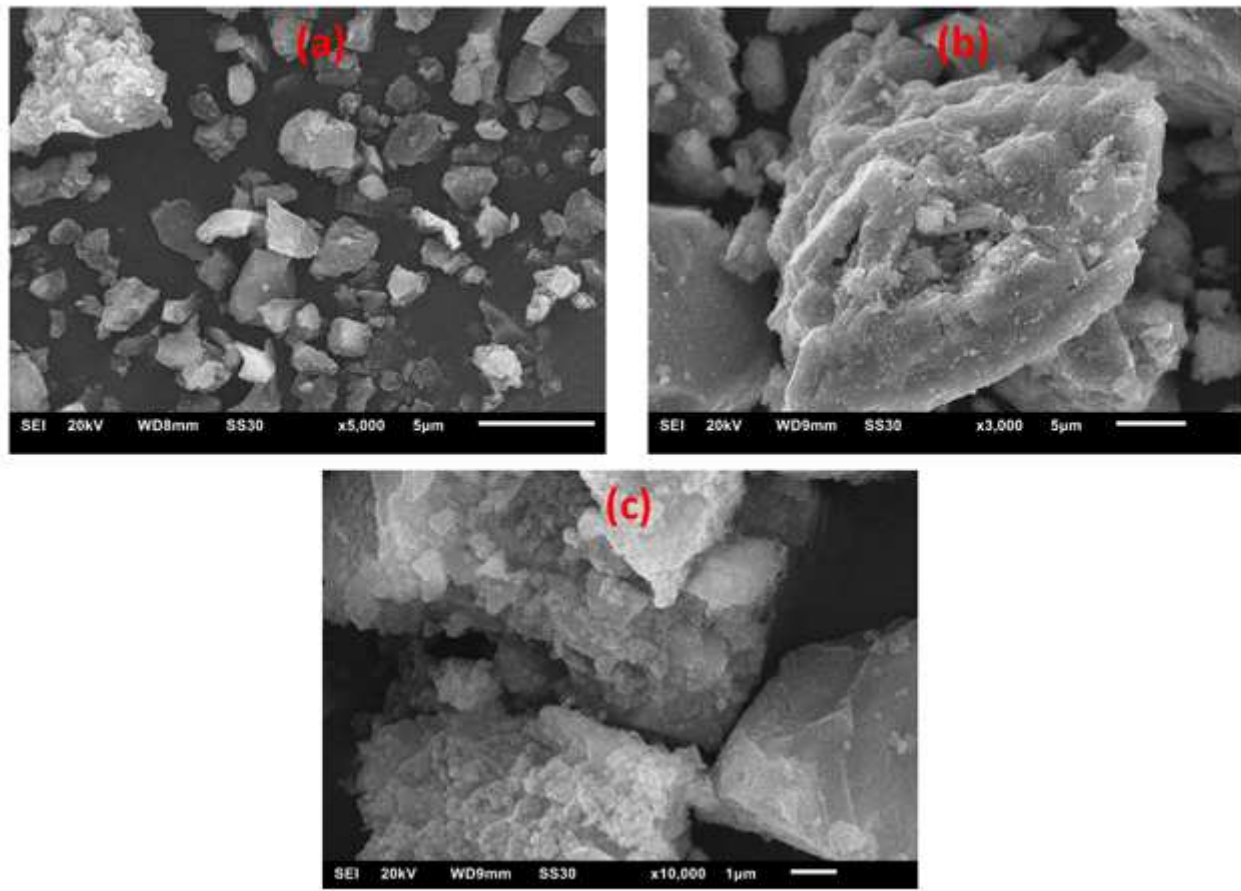


Figure 5

XRD patterns of precursor and GP0 and GP1 geopolymer

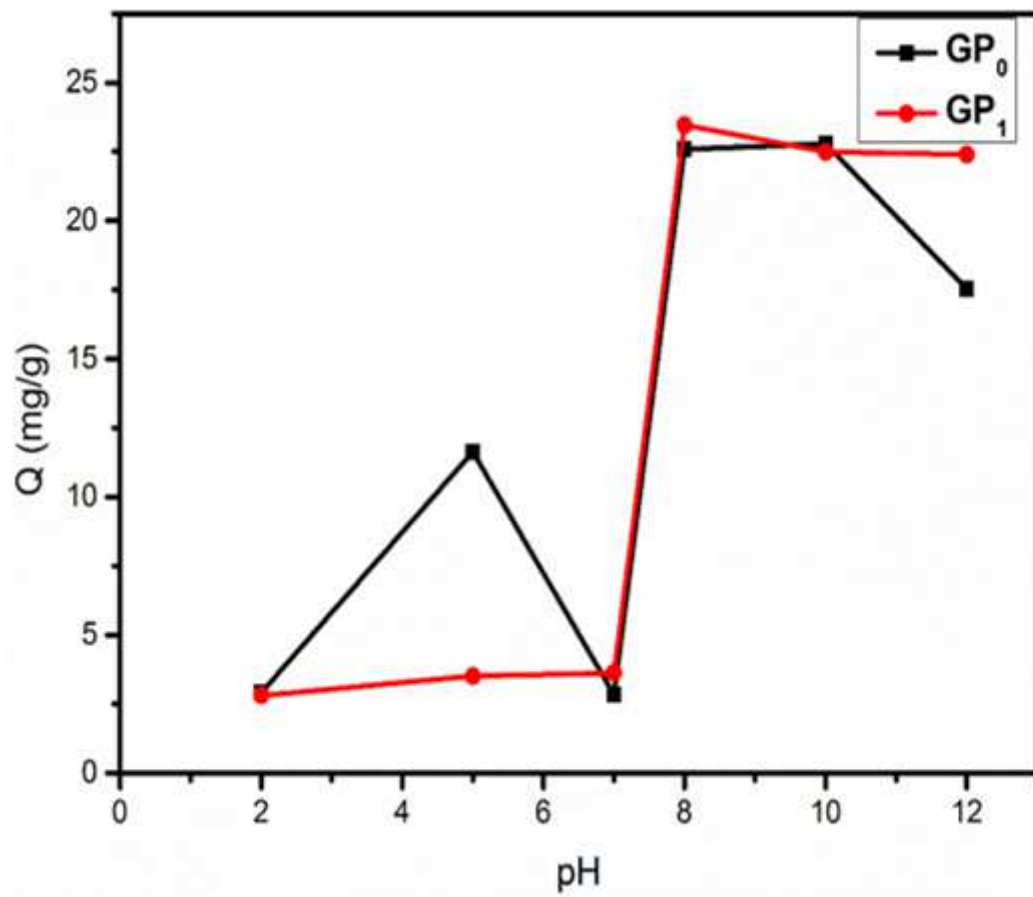


Figure 6

Influence of pH on the adsorption capacity of the different geopolymers.

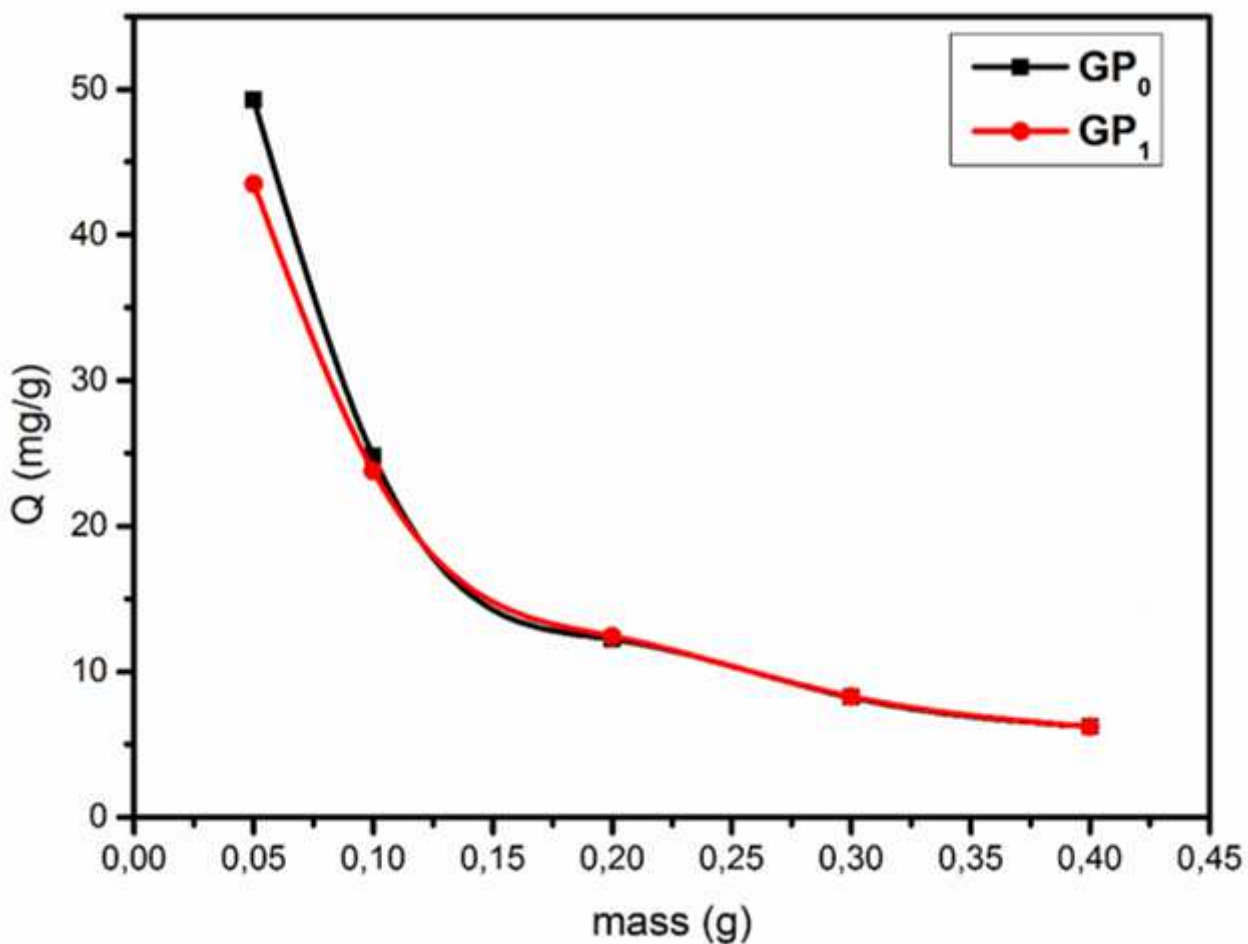


Figure 7

Influence of Adsorbent Dose

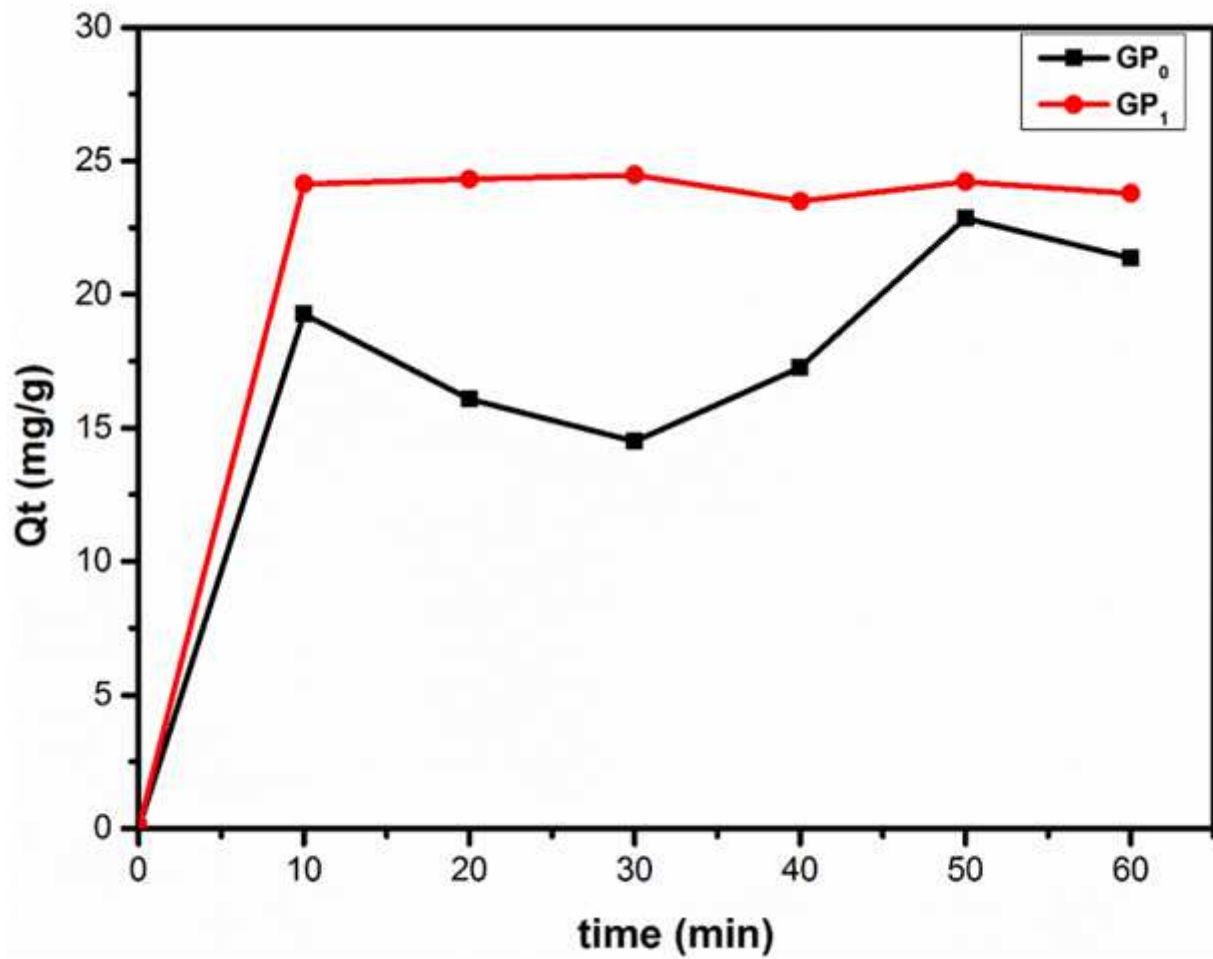


Figure 8

Effect of the MB contact time on the adsorption capacities of the different geopolymers

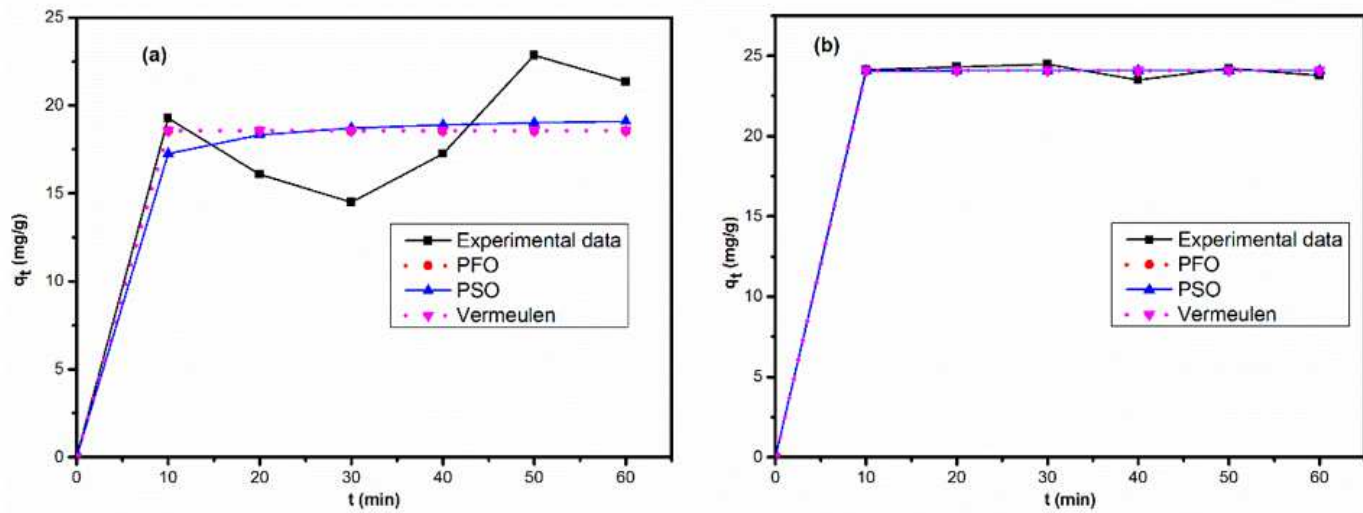


Figure 9

PFO, PSO and Vermeulen models applied to the experimental kinetic data for the adsorption of MB on different geopolymers ((a) GP0 and (b) GP1)

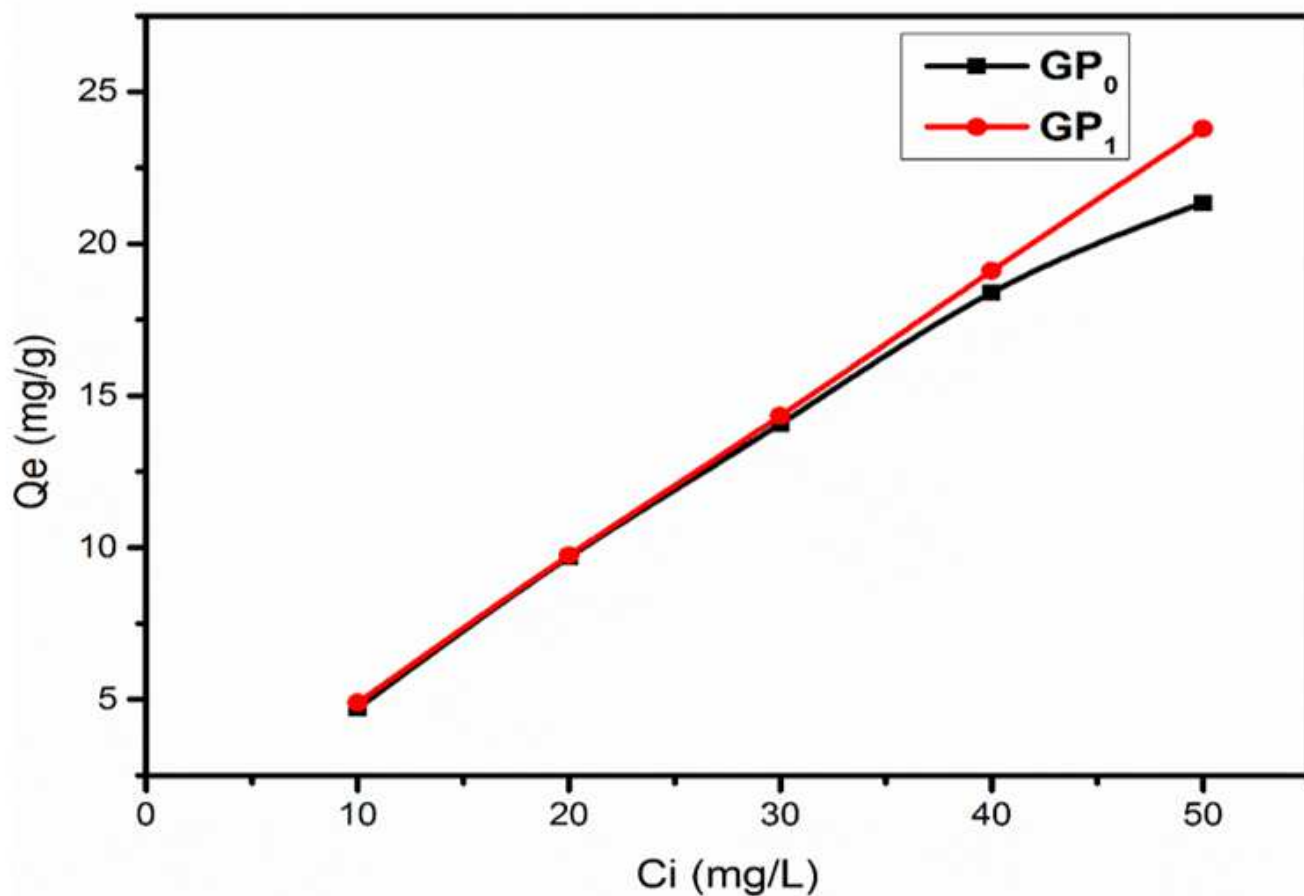


Figure 10

effect of initial concentration

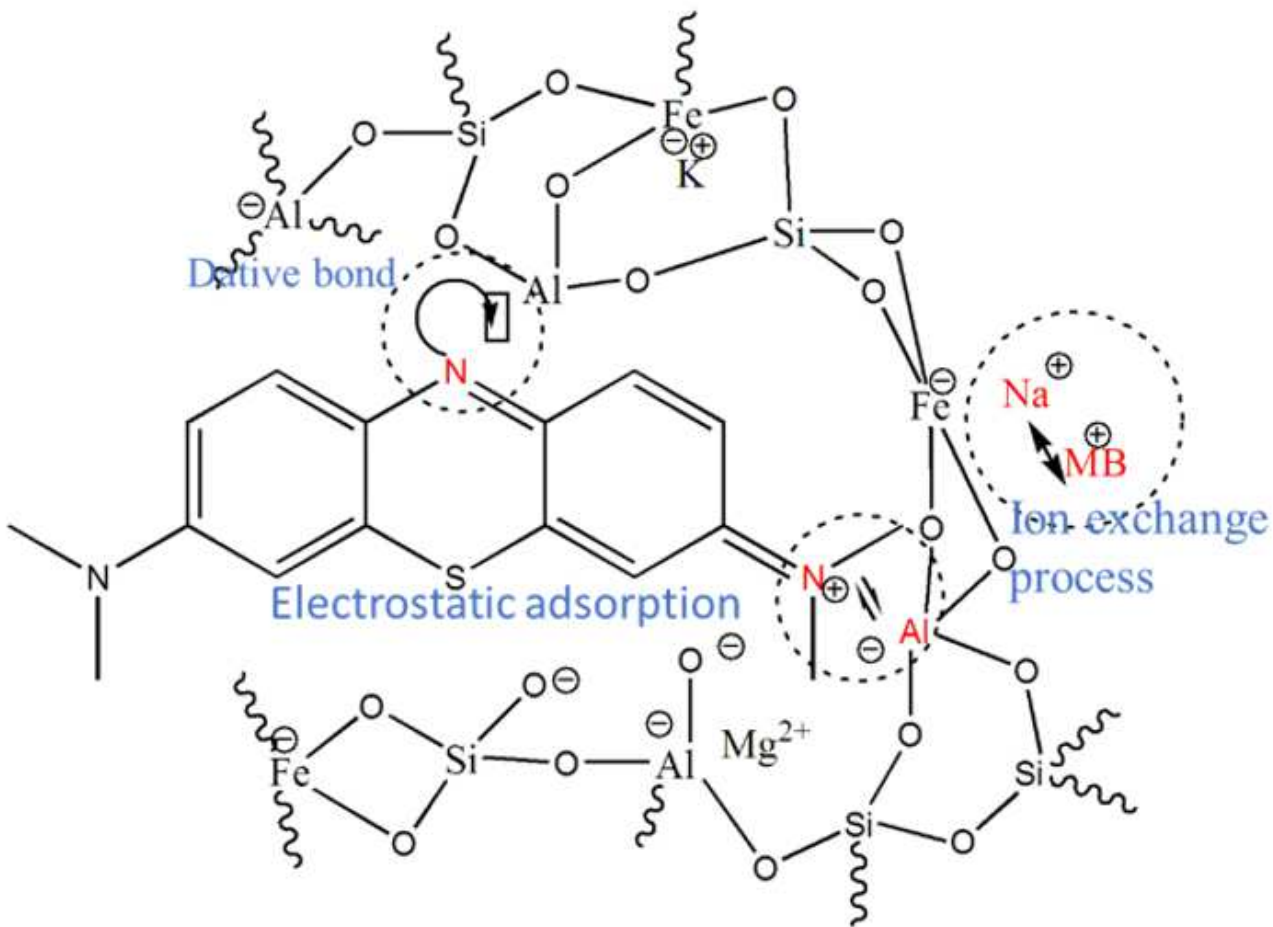


Figure 11

Interaction mechanisms in the GP1-MB system.

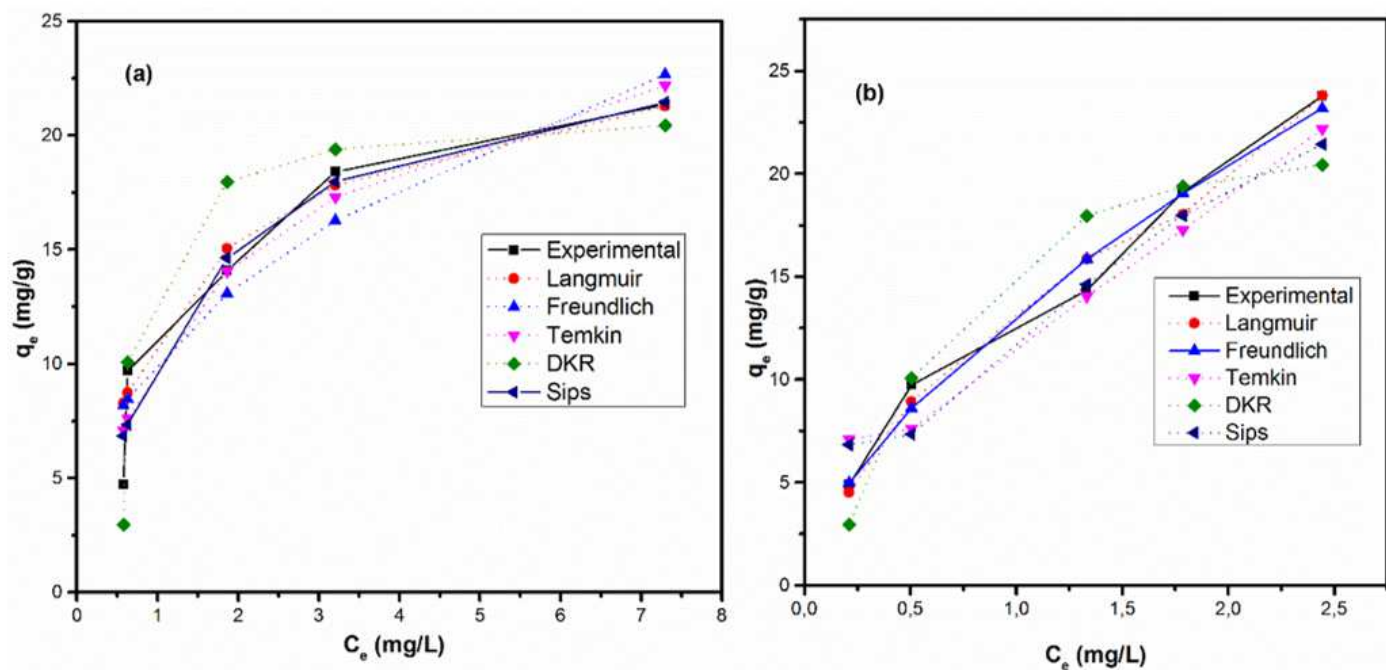


Figure 12

Adsorption isotherm plots for MB onto (a) GP0 and (b) GP1 materials

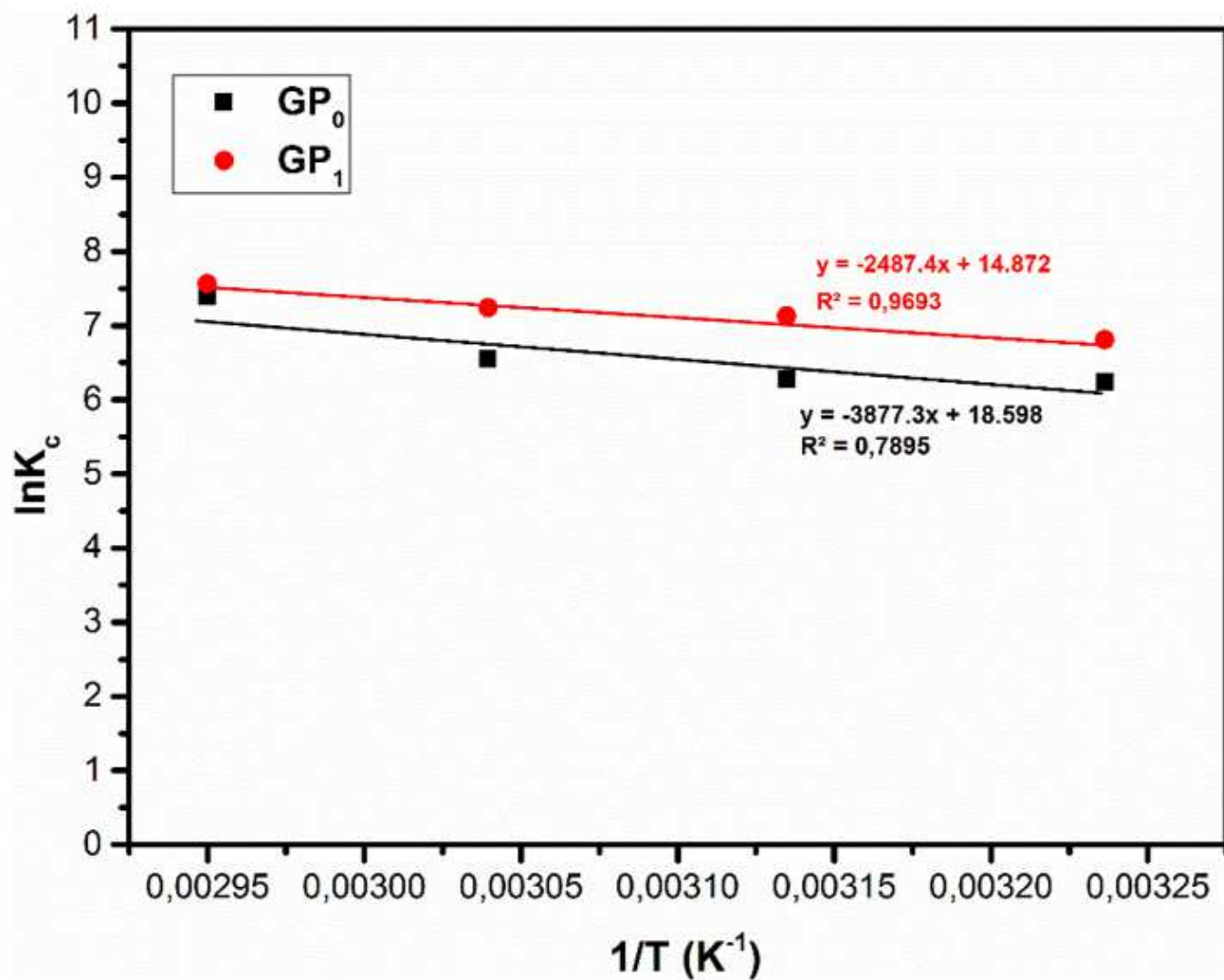


Figure 13

Isotherm plot of van't Hoff.

Supplementary Files

This is a list of supplementary files associated with this preprint. Click to download.

- [Graphicalabstract.docx](#)